Ambient Thin Film Water on Insulator Surfaces

George E. Ewing*

Department of Chemistry, University of Indiana, Chemistry Building, Bloomington, Indiana 47405

Received May 3, 2005

Contents

1. The Opening

Ambient liquid water always finds itself confined by one or more boundaries. For the water droplet, the boundary is the interface with its vapor. Sometimes two interfaces are involved, as in the case where the water is trapped in grain boundaries of ice. There are countless other examples of water confined by two interfaces whose geometry or separations can be controlled. In the case we shall consider, thin film water, there are also two interfaces. One is with the surface of its supporting substrate, the other is with its vapor. The film thickness is determined by the nature of the substrate, the water vapor pressure (or air relative humidity), and the temperature of the system. In general, we shall be talking about ambient conditions: near room temperature, say 20 ± 20 °C, and water vapor pressures corresponding to relative humidities from arid conditions up to 100%. The substrate surface can be either hydrophobic or hydrophilic.

When, as is often the case, the film has a thickness on the order of 1 nm, both the liquid−substrate and the liquid−vapor interfaces matter to the properties of the confined water. This makes the properties of thin film water both interesting and a challenge to understand. For the experimentalist, defining the substrate surface is difficult because, even if it is carefully prepared in a dry environment, it is likely altered by the introduction of water vapor. Almost all solids are soluble to a certain extent, and many substrate surfaces can chemically react with water. Water is, after all, not a passive liquid. The theorist is challenged by never being able to work with "real" water or the "real" substrate, but its representation as limited by a web of approximations.

* Phone: 812-335-5754. Fax: 812-855-8300. E-mail: ewingg@indiana.edu.

George Ewing has been educated by his parents, family, teachers, and friends (and not-so friends). He has received degrees from a number of accredited schools and joined the chemistry faculty of Indiana University in 1963. Over the years, he and his students have studied the chemical and physical properties of molecular complexes, liquids, surfaces, atmospheric particles, and ice. Thirty of these students have received Ph.D. degrees for their contributions to this research. Over 100 papers have resulted. Thousands of students have taken courses from him, and he has developed lectures for the general public on science. He is now Indiana University Chancellor's Professor Emeritus and continues research on thin film water and the properties of ice. He splits his time between Bloomington, IN, and East Machias, ME, where he is writing a book on ice.

We continue by considering why thin film water is worthy of study.

2. Overview

Thin film water is ubiquitous. It coats insulators, metals, semiconductors, and even ice under ambient conditions.[1] And the film can have a profound effect on the physical and chemical properties of the substrate it covers. There are many fundamental questions on the nature of thin films of water. How thick are they? What are their freezing points and abilities to dissolve molecules and ions? Are water molecules making up the film random or ordered? How are thermodynamic properties affected by the film thickness and the nature of the underlying substrate? What can be said about the hydrogen bonding network within a thin film on a hydrophobic (nonwetting) or hydrophilic (wetting) surface? How does chemistry within a thin film differ from chemistry in bulk water? In this review, we shall consider, by examining several model systems, some approaches to addressing these questions.

The properties of ambient thin film water are of great practical importance. Salt particles, thrown up from the earth's oceans, make up one of the most abundant particulate masses in the atmosphere.[2] Water coating their surfaces, sometimes called a quasi-liquid layer, affects chemical reactivity.[3] A thin film of water on aerosol particles in the

10.1021/cr040369x CCC: $59.00
Published on Web 03/25/2006

atmosphere is a likely prelude to cloud formation.[4] Small particles of a variety of solids (e.g., NaCl, detergents, fertilizers) manufactured annually in millions of metric ton quantities[5] cake together in clumps because of adhering water films, complicating their handling, packaging, and transport.[6] Thin film water participates in transformation of solids,[7] including mineral weathering and corrosion, and also affects the properties of soils.[8] Yet despite its relevance, the view of thin film water at the molecular level is incomplete.

Thin film water on ice deserves special consideration. The suggestion that a liquid-like water layer resides on the surface of ice at temperatures near its melting point dates to the work of Michael Faraday.[9] Interest in this thin water film, now variously called the premelting layer, surface melting layer, or quasi-liquid layer, has expanded over the years. Originally confined to understanding the properties of blocks of ice, snow, or glaciers, thin film water on ice is now implicated in the electrification of clouds[10] and interpretation of ice cores[11] and is involved in a vast array of environmental phenomena including frost heave, soil freezing, and permafrost.[12] Chemical transformation of ice crystals in polar snowpack[13] and stratospheric clouds[14] affects atmospheric ozone concentrations and is an interfacial phenomenon likely to involve thin film water. Heterogeneous ice nucleation begins at a solid interface with thin film water as intermediary.[4] Finally surface melting is now known to be a general phenomenon observed in many solids of which ice is perhaps the most complicated.[15] In short, the study of thin film water on ice continues to be a lively research area.

The subject of water interactions with surfaces is vast. A 1999 article in *Chemical Reviews* dealing with the aqueous influences on metal oxides alone required 13 authors.[16] This special issue of *Chemical Reviews* contains over a dozen contributions. Our review is then meant to be complementary. It is moreover restricted to only five substrates that each serve as model insulators to host thin film water. Three are ionic crystals: NaCl, MgO, and BaF_2. A fourth, muscovite mica, is held together by both covalent and ionic bonds. The fifth substrate is corundum, α-Al_2O_3, bound solely by covalent bonds. Two important classes of insulators have been ignored. One would be a hydrogen-bonded solid. Its representation by ice is covered in the discussion of its surface melting layer for this issue by Dash et al. The other insulator type ignored is van der Waals bonded as represented, for example, by the organic polymer polyethylene. The surfaces of these hydrophobic polymers should support water adlayers to a limited extent.

In the substrates we have selected, we have further decided to consider only well-defined faces: NaCl(001), muscovite mica (001), MgO(001), BaF_2(111), and α-Al_2O_3(0001). We have thus ignored the vast and important literature dealing with water adsorption on powders and crystallites covered by a number of texts. The important class of amorphous substrates, for example, glasses, has likewise been neglected. Our restrictive choices have been made, in part, because the well-defined surfaces can be reproducibly prepared and have been explored by a variety of experimental investigations and with detailed theoretical study as well.

We begin with a survey of methods for the study of thin film water.

3. Methods for Studying Thin Film Water

The study of thin water films on insulators started, as did many of the pioneering investigations in surface science, with Irving Langmuir.[17] In 1918, he measured water adlayers on mica and glass. His procedure, elegant in its simplicity, involved taking many sheets of mica or cover glass slides from the ambient laboratory environment and stacking them into a small vial. The adsorbed molecules (principally H_2O) on these surfaces were driven off by heating to 300 °C and captured in a trap cooled with liquid air. The number of water molecules caught, together with the known geometric area of the substrate surfaces, allowed a calculation of thin water film coverages: two molecular layers on mica and over four on glass. If we view these insulator substrates as typical, then we come to expect any insulator surface to have some water molecules stuck to it under ambient conditions.

Work since Langmuir on water adlayers has followed two distinct paths. With the development of ultrahigh vacuum (UHV) technology, thousands of studies of water on metal and nonmetal surfaces have been performed.[18,19] Typically water molecules on well-defined surfaces, as studied in an UHV environment, are locked into an ordered structure for long times (hours). The stability and order are dictated by the strength of the adlayer bond or the low temperature of the substrate. For example, a monolayer of H_2O has been prepared on a NaCl (100) surface under UHV conditions.[20] At -130 °C and a water vapor pressure of 10^{-8} mbar, helium atom scattering (HAS) diffraction and accompanying theoretical analysis has revealed an ordered adlayer with each Na^+Cl^- surface ion pair covered by a H_2O molecule at a specific orientation.

The path less traveled for water adlayer studies is for exploration of ambient thin films. With equilibrium pressures in the millibar pressure range, the scores of surface interrogation techniques, helium atom scattering and low-energy electron diffraction, X-ray photoelectron spectroscopy, etc., that depend on the low background pressures of the UHV chambers fail for ambient water thin film studies. However four particularly successful general approaches have been directed toward the investigation of ambient thin film water: intermolecular force measurements,[21−24] optical interrogations, both linear (e.g. ellipsometry[25−28] and infrared spectroscopy[29−34]) and nonlinear (second harmonic[35] and sum frequency generation[36−38]), and molecular simulations.[39−43]

Infrared spectroscopy has been a particularly valuable diagnostic for thin film water studies and provides two important levels of information. The first is from the spectroscopic signature, which can provide insight into the hydrogen bonding networks, particularly in the region of the ν_1 and ν_3 H_2O stretching modes. If there is no hydrogen bonding, that is, gas-phase H_2O, these modes are around 3700 cm^{-1}. In liquid water the absorption is near 3400 cm^{-1} and for ice about 3200 cm^{-1}. There are also accompanying changes in band shapes and optical cross sections. The second level of information is the determination of film thickness. For example, if the band shape indicates a liquid-like film, then the bulk liquid water optical cross section can be used to estimate the film thickness. These methods have been reviewed elsewhere.[1,31]

4. Thin Film Water Properties

4.1. Coverage and Thickness

We can use two measures to define the extent of the thin film on a surface. If we concentrate on the adsorption sites of the substrate surface, we can say that, on average, the coverage is submonolayer, monolayer, or multilayer. This

is the molecular view of the extent of the thin film. Alternatively, the water film can be viewed as a continuum with thickness measured between boundaries defined by the substrate surface and the beginning of the vapor region. To cast these two views into more visual expressions, consider Figure 1.

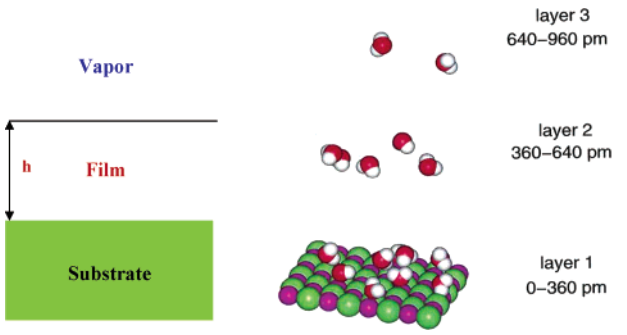

Figure 1. Models of thin film water: on the left the continuum model; on the right the molecular model. Reproduced with permission from ref 30. Copyright 2000 American Institute of Physics.

A thin film in the continuum model is represented on the left side of Figure 1. The film of thickness h is sandwiched between its vapor above and substrate below. The film is viewed as homogeneous and abruptly terminated at two interfaces: film−vapor and film−substrate. Clearly this is an idealized view since it implies that the interface is discontinuous. However, a physical interface separating phases cannot be discontinuous since the atoms, molecules, or ions that define it are described by wave functions, which are (in principle) infinite in extent. Moreover, the properties of one phase influence those of an adjacent phase, blurring the interface.[33] The transition from one to another becomes not a step function but a gently changing profile, whose descriptions go back to the work of Gibbs[44] and Drude.[45]

The molecular view of a thin film is taken from the work of Engkvist and Stone.[39] A finding from their Monte Carlo study of H_2O on NaCl(001) at 25 °C is presented on the right side of Figure 1. In this example, they have explored a coverage of $\Theta = 0.5$. We can interpret this value to mean that, on average, one-half of the Na^+ surface ions are covered by H_2O molecules. But in this exploded view, some molecules are against the NaCl(001) and other molecules extend away from the surface.

In the discussion to follow, some researchers describe a film by coverage, Θ, and others by thickness, h. It is useful to connect these two quantities by

$$h = \frac{\Theta S_R}{\rho_w} \tag{1}$$

where $\rho_w = 3.3 \times 10^{28}$ molecules m^{-3} is the density of bulk water at 25 °C[46] and S_R is the surface site density. For NaCl(001), this is 6.4×10^{18} ions (Na^+ or Cl^-) m^{-2}.[30] Using $\Theta = 0.5$ in Figure 1, we calculate $h = 0.1$ nm.

Neither Θ nor h make a satisfactory measure of thin film water. Since sites are only roughly covered in an ambient film, Θ makes only a crude quantitative description. And for a very thin, for example, subnanometer, film its density will not be homogeneous and will be much less than ρ_w. In addition, the interface boundaries are blurred.

For future reference, it is convenient to note that the effective packing diameter of a single water molecule is 0.28 nm, an average from crystallographic data,[22] and a monomolecular slice of bulk liquid water from $\rho_w^{-1/3} = 0.31$ nm.

4.2. Why Does a Thin Film Stick to a Surface?

Water is held near an insulator surface by energies that can usually be partitioned among five types: *electrostatic*, *dispersion*, *induction*, *repulsion*, and *hydrogen bonding*.[31,39] Taken together, these energies account for the phenomenon of water physisorption. In the following qualitative discussion of physisorption, we will concentrate on the example of H_2O on NaCl(001) with asides that will encompass other substrates.

The electrical properties of the water molecule include its dipole, quadrupole, and higher moments either located at a single site or distributed among a variety of sites within the molecule.[47] The dominant electrostatic interaction of H_2O with NaCl is by way of these electric moments and the electric field near the surface generated by the ions of the substrate. To appreciate the magnitude of this type of energy, consider first a H_2O molecule in the field of a single Na^+ ion. The field strength, in volts per meter (V m^{-1}), at distance z from the center of the ion is given by[48]

$$E = \frac{q}{4\pi\epsilon_0 z^2} \tag{2}$$

where $q = 1.6 \times 10^{-19}$ C is the elementary charge of Na^+ and $\epsilon_0 = 8.85 \times 10^{-12}$ C V^{-1} m^{-1} is the vacuum permittivity. Consider water and the ion at a separation defined by the touching of their hard sphere radii. We take this distance to be the sum of the Na^+ radius (95 pm[22]) and the H_2O radius (140 pm[22]) and arrive at $z = 235$ pm. Application of eq 2 yields an electric field of 2.6×10^{10} V m^{-1}. The energy of a dipole parallel to an electric field and favorably aligned[48] is

$$W(z) = -\mu E \tag{3}$$

and with $\mu = 6.2 \times 10^{-30}$ C m for H_2O,[48] we arrive at $W = -96$ kJ mol^{-1}. If we increase the distance of the molecule from the ion by the diameter of the water molecule, we arrive at a separation $z = 515$ pm to find $W = -20$ kJ mol^{-1}, still a considerable energy of attraction.

The electric field directly over an ion at the (001) surface of the collection of ions that make up a cubic face-centered ionic crystal is given by the Lennard-Jones and Dent expression[49]

$$E(z) = \frac{8\pi q}{4\pi\epsilon_0 a^2} \exp(-\pi\sqrt{2z/a}) \tag{4}$$

The separation z is measured above an ion of charge q, and the distance between nearest neighbor cation and anion is $a = 282$ pm for NaCl.[46] Comparison of eqs 3 and 4 shows that, while the decay of electric field from a single ion is quadratic with displacement, the decay is exponential from the surface of an ionic crystal. Using eq 4, we calculate $E = 0.8 \times 10^{10}$ V m^{-1} at $z = 235$ pm or roughly a factor of 3 smaller than for the same displacement from a single ion. The binding energy is comparably less, $W = -29$ kJ mol^{-1}. However, the big difference between interaction of the water with a single ion and a crystal surface comes about when we displace the water molecule again by its molecular diameter to $z = 515$ pm. This amounts to moving the

molecule touching the surface, that is, in the first layer, to the second layer. The exponential decay of the electric field results in a binding energy of −4 kJ mol^{-1}, a decrease by a factor of 7 over that for the molecule touching the surface. At a separation of 1 nm, the electrostatic binding is only −0.4 kJ mol^{-1}. And while we have greatly simplified the electrical properties of water and ignored the details of its orientation on the surface, this numerical exercise has provided two lessons. The first is that the binding energy of a water molecule at the surface of the ionic crystal is large and, as we shall soon show, comparable to a hydrogen bond energy. The second is that if the molecule resides in the second or higher layer, its electrostatic binding to the ionic substrate is negligible. Only the first layer is directly affected by the electric field of the substrate.

An estimation of the dispersion energy between water and the substrate is not so straightforward, but we can begin by considering the van der Waals interaction between a single water molecule and a single ion (or atom) within the substrate. The dominant attractive term in the two-body dispersion potential decays with displacement as z^{-6}.[47] If we now consider a water molecule near a surface, we must expand the number of participating ions (or atoms) by the substrate volume proportional to z^3.[22] As a consequence, the net attractive energy now decays only as z^{-3}, which might appear less severe than the exponential dependence of the surface electric field. And indeed it is, though the diminution of the dispersion energy when water moves from the first layer (z = 235 pm) to the second layer (z = 515 pm) is still an order of magnitude smaller. So as in the consideration of electrostatic interaction, the dispersion energy between a water molecule and the substrate is only significant when it resides in the first layer.

Since both repulsion and induction energies also depend on high powers of the displacement,[47] these two contributions to physisorption, like dispersion and electrostatics, will only influence the energetics of molecule−substrate interaction in the first layer.

To attach some quantitative numbers to the relative importance of the electrostatic, dispersion, induction, and repulsion energies, we refer to the calculations of Engkvist and Stone.[50] For a single water molecule atop the NaCl(001) surface, they find the electrostatic energy to be −57 kJ mol^{-1}, repulsion energy at 43 kJ mol^{-1}, induction energy of −13 kJ mol^{-1}, and a dispersion energy of −13 kJ mol^{-1}, for a net binding energy of −40 kJ mol^{-1}. The optimum structure they find, shown in Figure 2, has the water molecule positioned nearly above Na^+ and lying almost flat against the surface. This orientation, qualitatively different from the one we supposed in using eq 3, considers many electric moments of the molecule and the intricate variation of the electric field over the surface to achieve a 2-fold increase in electrostatic binding energy over our crude estimate. The net binding energy, −40 kJ mol^{-1}, is a compromise among the electrostatic term and the three other energy types, all with comparable values.

Before moving on to consider aggregations of water molecules on the surface of other insulators, it is helpful to consider the bonding within bulk liquid water. The enthalpy of condensation of water at 25 °C is −44 kJ mol^{-1},[48] and the formation of a single hydrogen bond in the liquid is estimated to be about −25 kJ mol^{-1}.[51] The numbers associated with hydrogen bonding energies are therefore comparable to the binding of water to an ionic substrate.

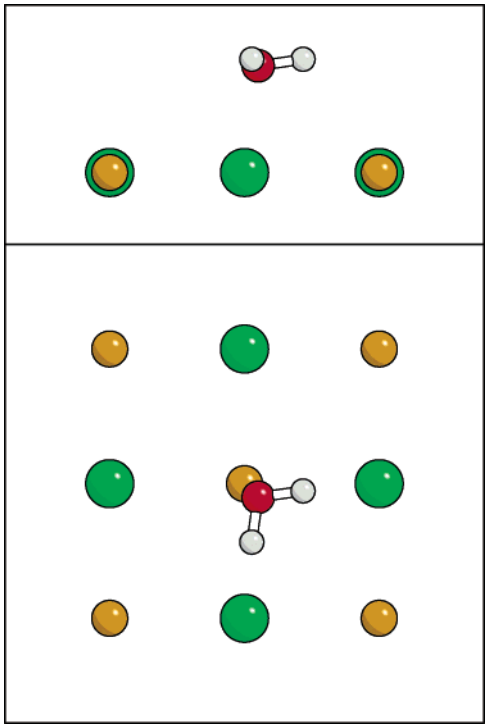

Figure 2. The structure of monomer H_2O on NaCl(001): bottom panel, top view with the small circles on the lattice Na^+ and the large circles Cl^-; upper panel, a side view. Reproduced with permission from ref 50. Copyright 1999 American Institute of Physics.

We can anticipate then that at least in the first adlayer of adsorbed water, hydrogen bonding within the film will be as important as bonding of the film to the substrate. For the second (or higher layers), the water molecules will not be affected *directly* by the substrate because the interactions fall off so rapidly with distance. However, water in the second layer will be affected by the water molecules in the first layer that are bound to the surface.

When we come to consider the bonding of the first water adlayer to a covalently bonded substrate, for example, α-Al_2O_3, it will greatly depend on whether the surface has been made hydrophilic by hydroxylation. The ability of a water molecule to participate in hydrogen bonding at the surface could compensate for the lack of electrostatic attractions that it would have with an ionic substrate.

While hydrogen bonding, electrostatic, dispersion, and induction add complexity to the structure of thin film water, repulsion alone can account for molecular layering. This is even evident in the distribution function for hard spheres against a hard surface.[51] Near liquid densities, the distribution function achieves a maximum as the first layer of spheres touch the surface. The second layer, in its turn, is restricted in its approach to the surface by the first layer and also exhibits a distribution maximum. Third and higher layers exhibit distinct, but decreasing, maxima as well. Layering of water against a hydrophobic surface has been demonstrated through various calculations[52] and for water against NaCl(001).[39]

4.3. Isotherms

Optical methods, such as ellipsometry and infrared spectroscopy can provide the thickness or coverage of thin film water on surfaces. The shapes of isotherms have been sources of information on adlayer or thin film structures since the work of Langmuir.[17]

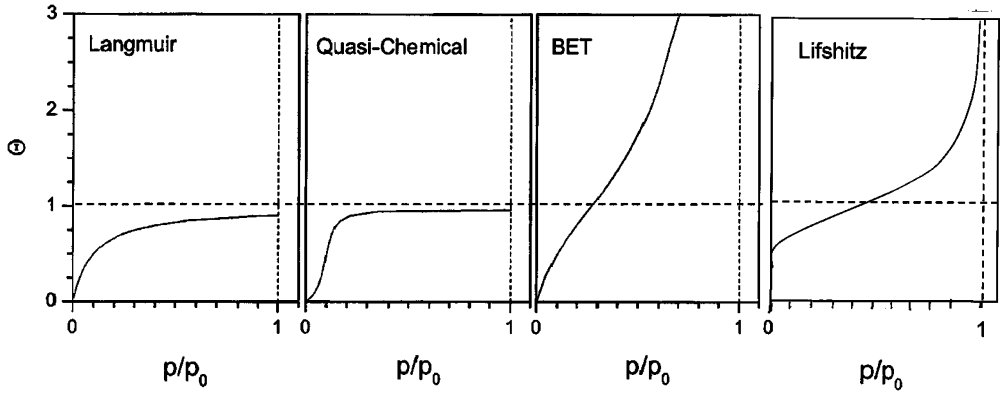

Figure 3. Model adsorption isotherms. Reproduced with permission from ref 31. Copyright 2003 Springer-Verlag.

The shapes of four model isotherms are given in Figure 3. Here p_0 is the bulk, equilibrium vapor pressure of water, and p its pressure over the substrate. In the first three of these presentations, we have arbitrarily taken $p/p_0 = 0.1$ for half monolayer coverage.

The simplest form, that from the Langmuir model,[17] follows from the view that adsorption occurs randomly to available surface sites. When all sites are filled, the surface is saturated by the monolayer and no further adsorption can occur. Lateral interactions are ignored and multilayer adsorption is denied. The cryogenic physisorption of CO on NaCl(001), for example, has been accurately represented by the Langmuir isotherm.[53]

The quasichemical model treats nearest neighbor lateral interactions through the parameter $nw/(kT)$.[54] The form of the resulting isotherm for $nw/(kT) = -4$ (i.e., an attractive interaction) is also shown in Figure 3. This isotherm is concave for low coverages with an inflection point at $\Theta = 0.5$. Above half-coverage, it becomes convex as it approaches saturation at $\Theta = 1$. The physical interpretation of the adlayer structure is that, at low coverages, molecules adsorb randomly and can be treated as a two-dimensional lattice gas. For high coverages, lateral interactions are responsible for two-dimensional crystalline island formations. A coexistence region at $\Theta = 0.5$ finds both lattice gas and crystal phases in the adlayer. At cryogenic temperatures, several small molecules[55] including H_2O[20] are well represented by the quasichemical isotherm. For H_2O on NaCl(001) near 100 K with the molecules nearly centered over Na^+,[50] they are separated too far for hydrogen bonds to form, so dipole attraction is the major lateral interaction. For these cryogenic studies, half-coverage occurs for $p/p_0 \ll 1$.

An *analytical* model that incorporates multilayer formation but ignores lateral interactions (e.g., $nw = 0$) is that of Brunauer, Emmett, and Teller (BET).[54] The model contains, within its parameters, the enthalpy of adsorption. An example of a BET isotherm (type III) is shown in Figure 3. The nature of the model allows multilayer formation as revealed by the asymptotic approach of multilayer formation as $p \rightarrow p_0$. Despite its denial of lateral interactions, many experimental systems are well represented by the form of the BET isotherm.

The Lifshitz model[22] is based solely on van der Waals attractions. The details of pairwise or many-body dispersion interactions are encompassed in the frequency-dependent dielectric constants of the media. Figure 1 represents this continuum three-layer model of the water thin film wedged between its vapor and the substrate to which it is bound. The collective properties for a particular system are quantified by the Hamaker constant A that may be calculated from the bulk optical/dielectric properties of the three-layer system or found listed in tables.[22] The analytical form of the Lifshitz model is remarkably simple, with film thickness given by

$$h = \left\{ \frac{A}{6\pi\rho_w kT[\ln p/p_0]} \right\}^{1/3} \quad (5)$$

We have plotted this form of an isotherm in the final panel of Figure 3 where we have taken $A = -5 \times 10^{-20}$ J, a value typical of water on a hydrophilic surface.[22]

Another revealing form of the measured isotherm is its behavior as $p/p_0 \rightarrow 1$. As discussed by Dash,[56] if the film is partially wetting, the coverage or thickness will terminate at some finite value as the water vapor reaches its equilibrium pressure. For a completely wetting surface, the coverage or thickness increases without limit as $p/p_0 \rightarrow 1$.

It is appropriate here to distinguish between adsorption and wetting. Wetting is a concept going back to the 19th century and the ideas of Young and Dupré.[21,22,48] In their continuum view, wetting was quantified by a contact angle that measured how a somewhat spherical drop rested on a substrate. The contact angle in turn depends on three (interfacial) surface tensions: liquid−substrate, liquid−vapor, and vapor−substrate. Adsorption, as we have presented the concept, is expressed in microscopic terms and involves the interaction of the first several molecular layers with the substrate. On this level, specific interactions involve the molecules with the substrate, molecules with each other, and molecules at the interface with the vapor. The convoluted details that connect these intermolecular interactions with the three surface tensions of Young and Dupré are beyond the scope of this review. Israelachvili has some lucid discussions connecting macroscopic and microscopic concepts in surface phenomena.[22]

4.4. Thermodynamic Quantities

Thermodynamic analyses of isotherms, taken over a range of temperatures, yield free energy, enthalpy, and entropy as a function of coverage. From these values, the changes in intermolecular bonding among the water molecules (the hydrogen bonding network) and bonding of water to the substrate can be assessed. In addition, it will be possible to gauge the ordering of water molecules on the substrate as a function of film thickness.

Extraction of thermodynamic quantities makes use of the expression[30]

$$\ln\left(\frac{p_0}{p_\Theta}\right) = \frac{\Delta H_w - \Delta H_\Theta}{RT} - \frac{S_w - S_\Theta}{R} \qquad (6)$$

where ΔH_w is the enthalpy of adsorption of liquid water (-44 kJ mol^{-1} at 25 °C)[48] and ΔH_Θ is the enthalpy of adsorption of the thin film at coverage Θ. The entropy of liquid water is S_w (70 J mol^{-1} K^{-1} at 25 °C),[48] and S_Θ is the entropy of adsorbed water at a coverage of Θ. In applying eq 6, we plot $\ln(p_0/p_\Theta)$ against $1/T$ using the appropriate value of the equilibrium bulk liquid water vapor pressure, p_0. When expressing the thin film in terms of its thickness, "Θ" replaces "h" in the above expression.

5. Some Systems

5.1. H_2O/NaCl(001)

NaCl(001) faces can be easily produced by cleaving a single crystal with a hammer and chisel. The surface structure exposed has Na^+ and Cl^- ions arranged in a square array. These surfaces have been examined by a variety of techniques[57−59] that show them to be atomically flat with occasional steps allowing smooth terraces for molecular absorption.

Water on NaCl(001) has been widely studied. For example, monolayer H_2O on NaCl(001) has been investigated near 100 K by helium atom scattering (HAS)[20] and low-energy electron diffraction (LEED).[60] At these cryogenic temperatures, each water molecule is locked into an energy minimum configuration for times on the order of hours. The resulting structures are monolayer crystalline arrays. By contrast, under ambient conditions (e.g., 0−30 °C and pressures of tens of millibars of water vapor), the lifetime of an adsorbed water molecule is easily calculated to be microseconds,[48] and the mobile adlayer structure is an ensemble of many irregular configurations, as we can see in Figure 1. Water adsorption has also been studied on the surfaces of NaCl crystallites.[61−64] However, since these defect-rich surfaces are poorly defined, the properties of adsorbed water layers are difficult to describe.

The infrared transmission approach to this model system, initiated in 1997 by Peters and Ewing,[29] has provided considerable insight into thin films on well-defined surfaces. In these experiments, a closely spaced stack of NaCl crystals with (001) faces exposed was placed in a temperature-controlled optical cell, which was set into the sample compartment of a Fourier transform infrared (FTIR) spectrometer that was then evacuated. The small spaces between the crystal slabs and the presentation of many faces minimized the interfering absorption by the vapor and maximized absorption by adsorbed water.

The spectra reveal a diffuse absorption associated with the vibrational stretching region of water molecules within the films on the NaCl(100) surfaces. For example, the infrared absorption spectrum of thin film water on NaCl(001) at 24 °C and 12 mbar taken from later work[30] is shown in Figure 4 and compared with the calculated spectroscopic signatures of 5 M brine[65] and bulk water.[66] The close similarity of the neat water or brine profiles with monolayer ($\Theta = 1$) water is good evidence that the thin film is liquid-like. Use of the optical constants of liquid water and the Beer−Lambert relation enabled the $\Theta = 1$ coverage value for 12 mbar in Figure 4; other coverage values at a range of pressures allowed construction of the isotherm in Figure 5. To provide a context with an ambient environment, the water pressure needed to produce a monolayer on NaCl(001) corresponds to 40% relative humidity (RH), a rather arid condition.

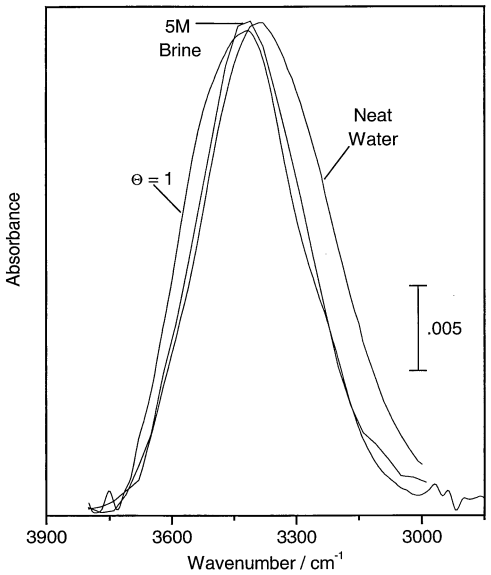

Figure 4. Infrared spectra of a monolayer of water on NaCl(001) at 25 °C together with calculated profiles of neat water and brine. Reproduced with permission from ref 30. Copyright 2000 American Institute of Physics.

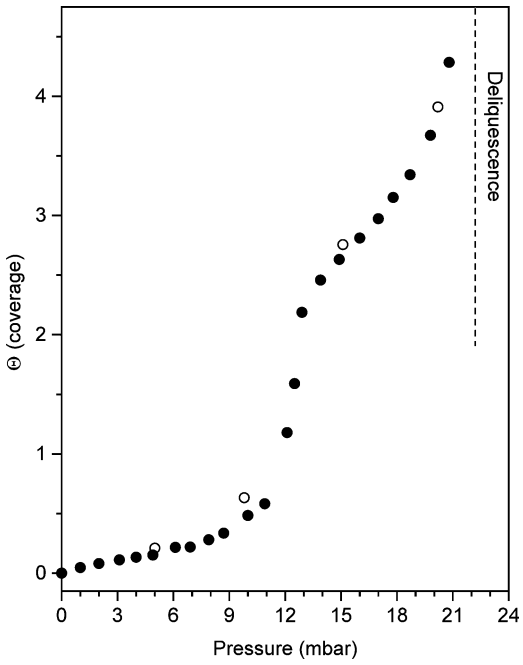

Figure 5. Isotherm of thin film water on NaCl(001) at 24 °C. Data taken on ascending and descending pressures are given by closed and open circles, respectively. Reproduced with permission from ref 30. Copyright 2000 American Institute of Physics.

The isotherm for water on NaCl(100) in Figure 5 is rich in detail, its interpretation aided by the Monte Carlo calculations of Engkvist and Stone. At a coverage of $\Theta = 0.5$, two-dimensional islands form with H_2O molecules hydrogen bonded both to each other within the island and also to the surface. The panel on the right of Figure 1 has given the results of this calculation as a "snapshot" of a typical configuration.

More quantitative expressions of the molecular nature of the thin film are in the pair distribution functions, $g(z)$, shown in Figure 6 for $\Theta = 0.5$ and $\Theta = 3.0$. Some details of these

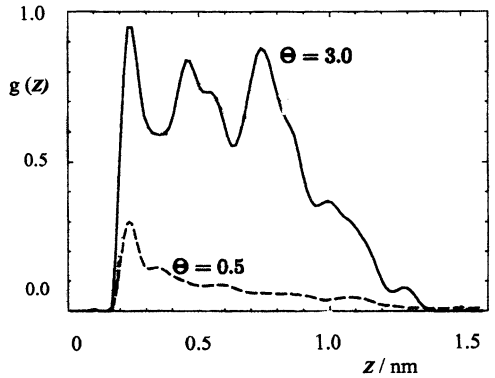

Figure 6. Distribution function $g(z)$ of water molecules at distance z from the NaCl(001) surface at coverages of $\Theta = 0.5$ and $\Theta = 3.0$. Reproduced with permission from ref 39. Copyright 2000 American Institute of Physics.)

distribution functions are revealing. For the submonolayer coverage, $\Theta = 0.5$, not all the molecules are stuck to the surface but spill out away from it. This was evident in the Figure 1 presentation. For multilayer coverage, $\Theta = 3.0$, there is distinct layering with three (nearly) regularly spaced maxima shown for $g(z)$. But in addition water molecules populate the region beyond the third maximum fading out only slowly beyond 1.1 nm or about four molecular diameters. What appears to be a phase transition occurs between $\Theta = 1$ and $\Theta = 3$ where the hydrogen bonding network now extends between layers of molecules as the film thickens. The transition then is from a two-dimensional film to a three-dimensional film. The onset of deliquescence, the spontaneous dissolution of NaCl at 23 mbar, is signaled in the isotherm by the abrupt increase in coverage above $\Theta = 4$.

Foster and Ewing[30] have measured a family of isotherms. From the changing coverage values with pressure and temperature, they have been able to extract thermodynamic quantities (ΔF, ΔH, ΔS) that characterize thin film water for H_2O on NaCl(100). For example, the enthalpy of vapor condensation to form the monolayer film is $\Delta H = -50$ kJ mol^{-1} or more exothermic than that for the condensation to liquid water, which is -44 kJ mol^{-1}. The monolayer film entropy at 55 J K^{-1} mol^{-1} is 15 J K^{-1} mol^{-1} lower than that for liquid water. In summary, water molecules are more strongly bound to the NaCl(100) surface than in the liquid and are more ordered.

The infrared study of H_2O/NaCl(001) we have just reviewed and the calculations by Engkvist and Stone have conveniently side-stepped the issue of the dissolution of the substrate even before deliquescence. However, the early work by Hucher et al.[67] and later atomic force microscopic studies[68−73] clearly point to water-induced surface changes at low relative humidities. Shindo et al.[68] have measured step migrations at relative humidities just above 40% RH, which coincide with a rise in surface electrical conductivity and step pattern changes recorded by transmission electron microscopy by Hucher et al. Impressive evidence for thin film water induced surface changes is a consequence of scanning polarization force microscopy (SPFM) measured by the group of Salmeron.[69−73] In this technique, the microscope tip is charged relative to the surface it is interrogating. The resulting changes in force respond to polarization of the surface including its thin film of water.

An example of their study[73] of H_2O/NaCl(001) is shown in Figure 7. The upper panel shows a SPFM topographical

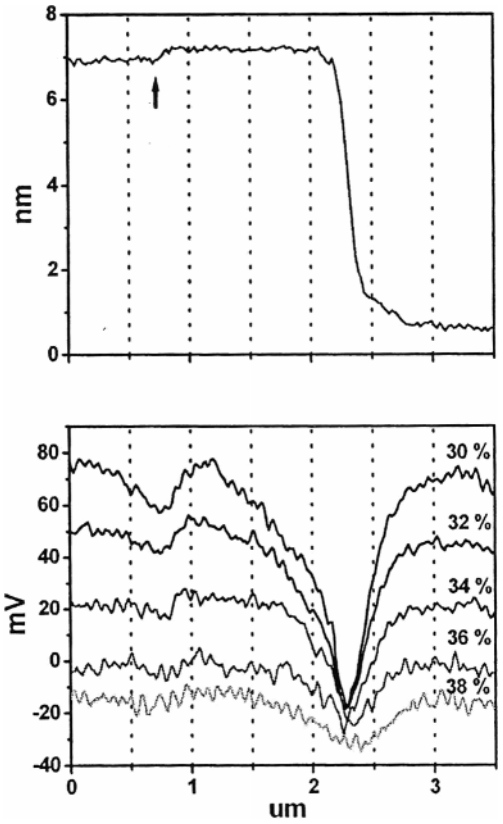

Figure 7. Scanning polarization force microscopy of the H_2O/NaCl(001) surface at 25 °C: top, topographic profile showing multiple step 6.5 nm high and monatomic step (marked by the arrow) at 30% RH; bottom, contact potential of the same area for different relative humidity values. Reproduced with permission from ref 73. Copyright 2005 American Institute of Physics.)

profile of a region of the NaCl surface at 30% RH. The arrow indicates a monatomic step (0.26 nm) with a uniformly smooth terrace on the right then dropping through a multiple step of 6.5 nm to another smooth terrace. The smooth terrace on NaCl(001) in this region is on the order of 1 μm wide. The lower panel of Figure 7 shows the electrostatic contact potential of the same area for different humidity values. At 30% RH, the electrostatic potential was $+75$ mV over the terraces. The monatomic step potential (60 mV) and multistep potential (-10 mV) were more negative than the terraces. On increase of the humidity, the electrostatic potential smooths out and appears to approach a uniform value of about -20 mV. In the terrace regions, the authors suggest that the initial negative values of the steps at low humidity are due to Cl^- solvation in the region of the steps. Increasing humidity causes the Cl^- solvation to spread out over the terraces. It is important to note that there is not step movement in these images. The single and multiple step positions do not change from 30% to 38% RH in Figure 7. The authors report that the solvation is reversible for humidities less than 40% but for high values step movement sets in and the surface is irreversibly changed.

We leave this exceedingly complicated system with many questions unanswered.

5.2. H_2O/Muscovite Mica (001)

Muscovite mica has been a popular substrate for the investigations of thin film water. Its structure is that of

stacked layers held together by electrostatic forces. The details of the complicated architecture are clearly described by Pauling.[74] The atomic assay is $K^+[Al_2(Si_3Al)O_{10}(OH)_2]^-$ with the negative layer a tetrahedral network of aluminosilicates. Pairs of negative layers are held together by K^+ ions. Muscovite mica is easy to cleave into atomically smooth sheets. The aluminosilicate portion remains intact and the K^+ ions become divided onto the newly formed (001) faces. The positive ion partitioning is never quite even, and each sheet initially is electrostatically charged.[75] These charges soon dissipate as bits and pieces from the ambient laboratory surroundings settle on the surfaces and neutralize them. While easy to prepare, the muscovite mica (001) faces are difficult to keep clean. So the experimentalist has the challenge of preparing and maintaining pristine and defect-free surfaces. On their side, the theorists can never work with real mica or pure water but only their representation by the intermolecular potentials they select, the quantum mechanics approximations, and the system size.

Mica has an affinity for water, and its study since the 1918 work of Langmuir[17] remains the subject of some ambiguity. Following Turnbull and Vonnegut's conjecture that a close match between lattice constants of ice and a substrate might facilitate the liquid water−ice phase transition,[76] Jaffray et al.[77] and Bryant et al.[78] investigated mica as a possible candidate as an effective ice nucleating agent. Water molecules adhering to mica should already be in a configuration close to the crystalline structure of ice, reducing the degree of supercooling necessary to induce nucleation. However, mica does not initiate nucleation until the water is supercooled to −10 °C.[4]

The thickness of water film as a function of relative humidity near room temperature has been measured by ellipsometry. Beaglehole et al.[79,80] determined that water wets mica incompletely. They inferred a coverage of one statistical monolayer at 75% RH. In contrast, Miranda et al.[81] concluded that a monolayer was formed only as the relative humidity approached 90%. Though it clouds the picture even further, it should be noted that Elbaum and Lipson[82] reported that water wets mica completely.

Consider now the 18 °C isotherm of thin film on mica constructed by Beaglehole et al.[79] shown in Figure 8. The authors note that the linear behavior at low coverages is consistent with the suggestion that adsorption is driven by entropy effects. In other words, a water molecule adsorbs independent of whether a neighboring site is occupied. This view is tantamount to denying the importance of lateral interactions such as hydrogen bonding. The linear regions of both the Langmuir and BET isotherms for low coverages as shown in Figure 3 are also a consequence of ignoring lateral interactions. The finite thickness at saturation, about 2.5 nm from Figure 8, is consistent with the authors' finding that the contact angle is ∼6° to 7° rather than 0° for complete wetting.

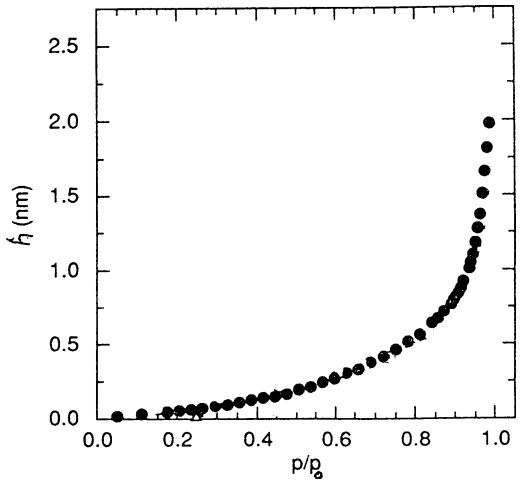

Figure 8. Isotherm of thin film water on muscovite mica (001) at 18 °C. Reproduced with permission from ref 79 (http://link.aps.org/abstract/PRL/v66/p2084). Copyright 1991 American Physical Society.

The lack of evidence for layering in the observed smooth isotherm of Figure 8 and the suggestion that the water interactions are nonspecific suggests the possibility that the Lifshitz theory could account for the observations. But alas the form of the Lifshitz isotherm, based on van der Waals forces alone, does not fit the observed isotherm behavior.

A thermodynamic description of thin film water on mica has been provided by Cantrell and Ewing[33] using infrared spectroscopy to yield coverage information using the same procedures that generated Figure 4. Their room-temperature isotherm resembles that in Figure 8. But extending their study over a range of temperatures from 0.6 to 25.1 °C, they could extract thermodynamic quantities making use of eq 6. Figure 9 shows the enthalpy of adsorption and absolute entropy of the adsorbed water as a function of coverage. The dashed line in both panels of the figure delineates the values for bulk water. The error bars in coverage are derived from the uncertainty in absorbance determinations. The error bars in enthalpy and entropy arise principally from uncertainties in the pressure as a function of the coverage.

The condensation of water onto mica is exothermic at all coverages with an extremum at approximately $\Theta = 1$ as shown in Figure 9. In the model that describes intermolecular bonding of water in the liquid phase,[83,84] each molecule is in a roughly tetrahedral hydrogen bonded arrangement with its neighbors. At submonolayer coverages, most molecules bonded to the surface are not fully tetrahedrally coordinated. Cantrell and Ewing visualized this situation as islands of water molecules scattered across the mica. Water molecules on the periphery of these islands will lack neighbors with which to form intermolecular bonds, that is, they will have dangling bonds. As more water adsorbs, near $\Theta = 1$, the clusters begin to coalesce resulting in an increase in the enthalpy of condensation because water molecules can bond not only to the surface of the mica but to neighbors laterally as well.

The entropy of adsorption mirrors the change in enthalpy. At the very lowest coverages, the water molecules are even less ordered than those in bulk water. This is demonstrated in the lower panel of Figure 9 where the entropy of the thin film near $\Theta = 0.2$ actually exceeds that of the liquid. This may be a consequence of configurational entropy[54] because the islands containing small numbers of water molecules are randomly dispersed across the surface of the mica. As more water molecules are added to the surface, they are "locked" into position by their neighbors. The entropy decreases to a minimum near $\Theta = 1$ implying the most ordered adlayer arrangement.

The extrema in the enthalpy and entropy at $\Theta = 1$ are possibly a consequence of the thin film structure described by Miranda et al.[81] as an ice-like layer. Measurements of the conductivity of water adsorbed to mica have also suggested the presence of a structured first layer.[85] Significantly, the decrease in entropy between bulk water and the entropy for $\Theta = 1$ is 23 ± 7 J K^{-1} mol^{-1}. The change in entropy for

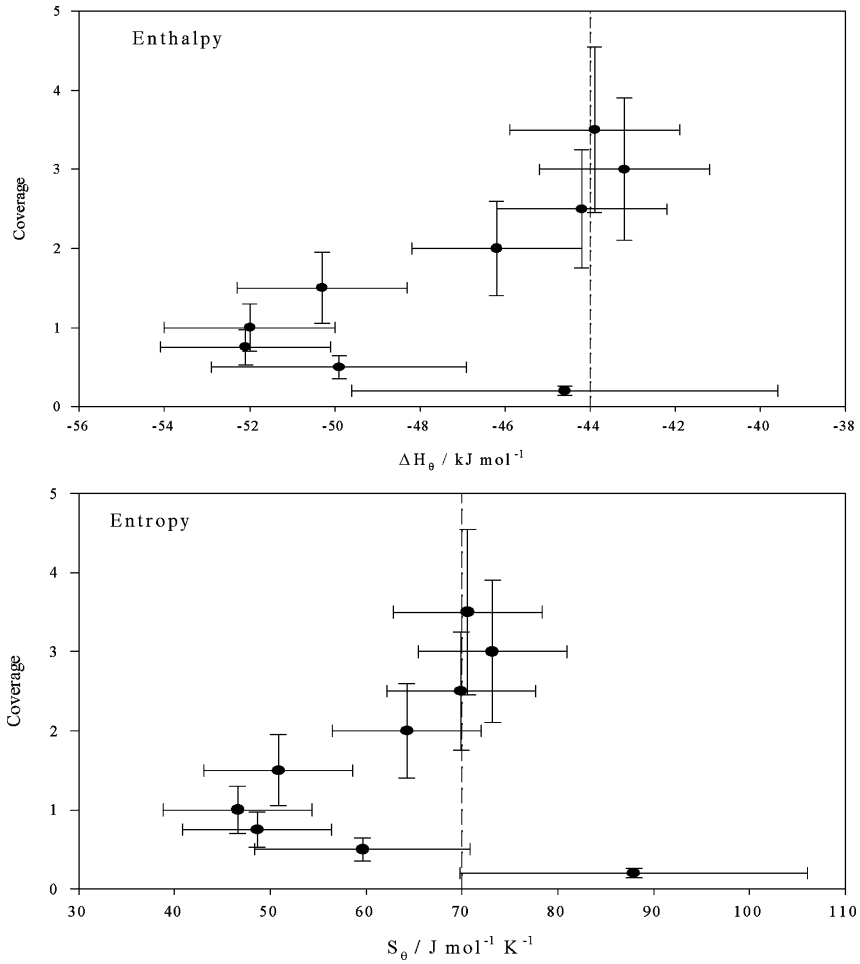

Figure 9. Enthalpy and entropy of thin film water on muscovite mica (001). The dashed line in the upper panel marks the value of the enthalpy of condensation of liquid water from the vapor at 25 °C. The dashed line in the lower panel marks the absolute entropy of liquid water at 25 °C. Reproduced with permission from ref 33. Copyright 2001 American Chemical Society.

the liquid to crystalline phase transition for bulk water at 0 °C is 22 J K^{-1} mol^{-1}.[48] The absolute entropy of the adsorbed monolayer is therefore comparable to that of bulk ice.

Odelius et al.[86] have explored thin film water on mica through a molecular dynamics (MD) calculation using an ab initio density functional framework. They arrive at a two-dimensional hydrogen bond network in registry with the underlying (001) mica surface as shown in Figure 10. This solid-like phase resembling a slice of the I_h ice structure is stable at room temperature and is consistent with the thermodynamic analysis.

As the coverage increases, $\Theta > 2$, the enthalpy and entropy approach those of bulk water, indicating that the thickness of the film is increasing beyond the range of the substrate forces. As the influence of the mica is reduced, the water molecules behave more like molecules in the bulk.

The dynamic behavior of water films on mica has been investigated by Elbaum and Lipson[82] by using an interference microscopic technique. A wetting layer of water, 1 μm or more thick, is first formed on the mica surface. When the temperature is raised, water evaporates and the film thins. In the region of a few tens of nanometers, the film becomes unstable and "dry" patches form on the mica.

Salmeron and his group have extended these studies of dynamic water films on mica using SPFM.[81,87] The nonequilibrium conditions are set not by evaporation as in the approach by Elbaum and Lipson but by capillary condensation on the SPFM probe tip. On removal of the tip from a freshly cleaved mica surface in a humid environment, images such as those shown in Figure 11 are observed.[87] Initially water islands (the white patches in the SPFM images) form. And as evaporation proceeds, moving from upper left to lower right in Figure 11, the islands disappear leaving a water monolayer. Analysis of the boundaries of these islands found a preponderance of angles of 120°, suggesting ice-like structures.

An extensive MD calculation by Wang et al.[88] using a relatively large system (eight crystallographic surface unit cells and up to 319 adsorbed water molecules) was able to explore films up to 3 nm. In agreement with the work of Odelius et al.,[86] they find a stable surface structure for a full monolayer coverage but not two-dimensional or ice-like. There was orientational order of the lower water layer with their molecular dipoles directed toward the surface in agreement with the calculations of Odelius. For molecules near the film−vapor boundary, the dipoles tended to be aligned along the interfacial plane allowing some non-hydrogen-bonded structures. This dipolar behavior is consistent with the findings of sum frequency generation (SFG) studies,[81] which show dangling (non-hydrogen-bonding) hydrogens at the film−vapor interface but not for water molecules next to the surface.

The atom density profiles measuring the oxygen and hydrogen atoms of water as a function of its distance from the surface calculated by Wang et al.[88] are shown in Figure 12. Of note is the distinct layering, up to five maxima at $\Theta = 3.38$. But unlike the distribution for water on NaCl(001)

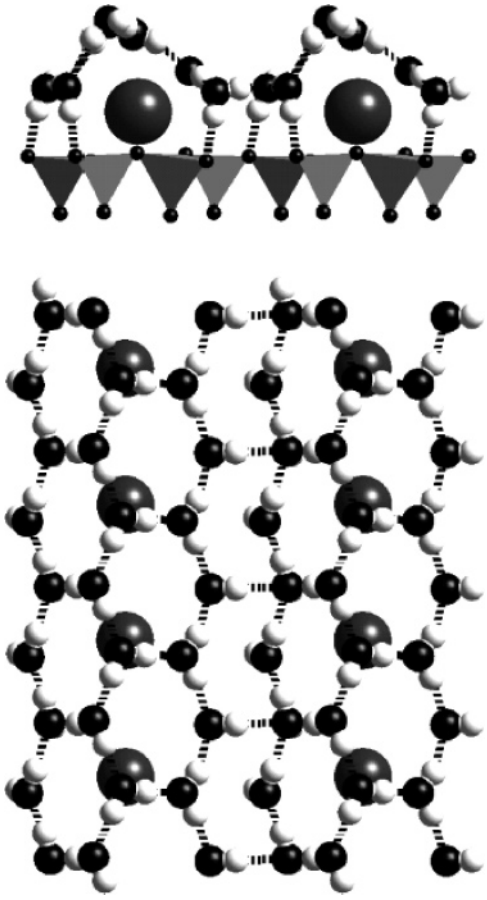

Figure 10. Optimized structure of monolayer water on muscovite mica (001) from molecular dynamics simulations. Reproduced with permission from ref 86 (http://link.aps.org/abstract/PRL/v78/p2855). Copyright 1997 American Physical Society.

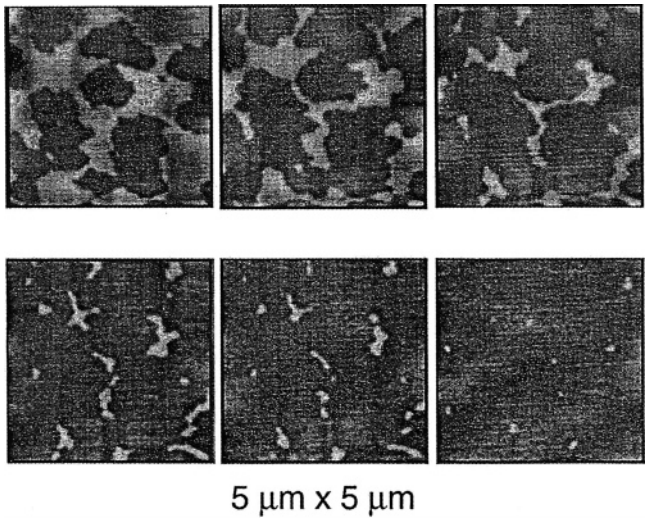

Figure 11. Evolution of scanning probe force microscopy images of water structures on muscovite mica (001) during drying. Reproduced with permission from ref 87. Copyright 1998 American Chemical Society.

at a similar coverage, see Figure 6, the oxygen spacings are irregular. At $\Theta = 6.65$, a slight increase (3%) in atomic density at 25 Å is interpreted as a response to the hydrophobic nature of the vapor interface.[88]

5.3. H_2O/MgO(001)

The surface science of metal oxides is well investigated, the subject of at least one book,[89] and their interactions with water were surveyed in recent reviews.[16,90] Magnesium oxide has received special attention for a variety of reasons. To begin, MgO has an aesthetic appeal of being, like NaCl, a face-centered cubic crystal and revealing on cleavage a (001) face with a square lattice. The interaction of MgO(001) with water has inspired a number of theoretical studies that suggest that H_2O physisorbs to terraces and dissociatively reacts at defect sites.[91−95] Some experiments have demonstrated molecular adsorption,[96−99] while others provide evidence for dissociation.[100−105]

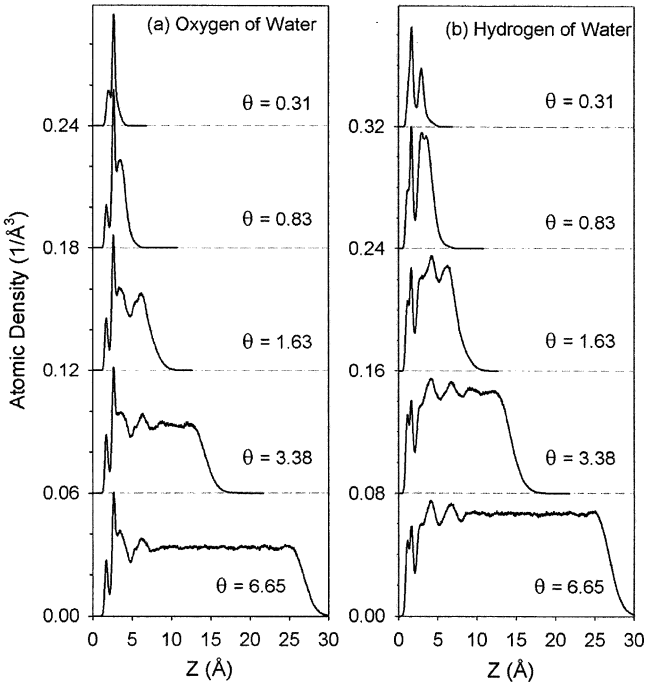

Figure 12. Atomic density profiles of water on muscovite mica (001). Reproducedwith permission from ref 88. Copyright 2005 American Chemical Society.

Before looking in detail at any experimental approach or theoretical calculation for the fate of water on MgO, we can anticipate some results. The electric fields near the MgO(001) surface should be much larger than those near NaCl(001) for two reasons. The Lennard-Jones and Dent relationship, eq 4, shows the importance of two substrate parameters: the lattice constant, a, and the ionic charge, q. The lattice constant is much smaller for MgO than for NaCl, and the ionic charges for MgO are ± 2[93] and those for NaCl ± 1.[50] These two parameters operate in directions that favor a larger electric field over the anions (or cations) of MgO than NaCl. The electrostatic contribution would therefore favor strong electrostatic binding of H_2O to MgO. Other factors come into play as well, and the final theoretical result using the approach by Engkvist and Stone gives the bonding of monomer H_2O onto MgO(001) as -65.4 kJ mol^{-1},[93] significantly greater than -40 kJ mol^{-1} for H_2O on NaCl(001).[50] The arrangement of H_2O on MgO(001) is qualitatively similar to that of H_2O on NaCl(001) that we have shown in Figure 2. Monolayer structures on both substrates are likewise similar in arrangement. But of course what we care about in this review are not adlayers at essentially a 0 K calculation but those under ambient conditions.

The approach adopted by Foster and her group reveals many of the properties of thin film water MgO(001).[106−108] The infrared spectra in the −OH stretching region over a range of pressures at 10 °C are shown in Figure 13. The

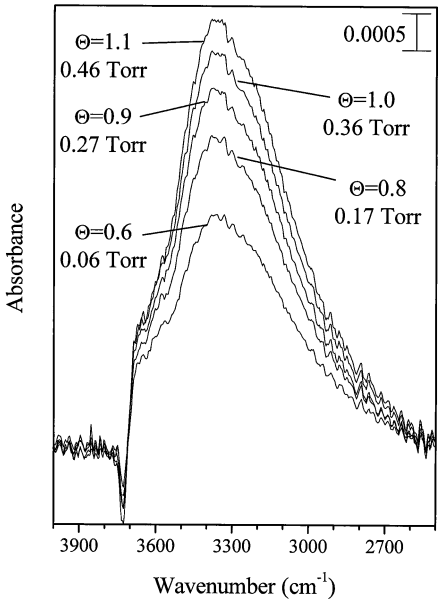

Figure 13. Infrared spectra of water on MgO(001) at 10 °C. Reproduced with permission from ref 108. Copyright 2005 Elsevier.

techniques used in obtaining these spectra were essentially the same as those we have described for infrared studies of H_2O on NaCl(001). For both substrates, the thin film band centers and bandwidths are close to those of liquid water. However a unique characteristic of the infrared signature of water on MgO(001) is the sharp absorbance deflection near 3700 cm^{-1}. Nevertheless, assuming that the liquid water optical constants can be used to determine coverages for the thin films, they are noted in Figure 13, and the resulting isotherm is presented in Figure 14. A slight hysteresis is

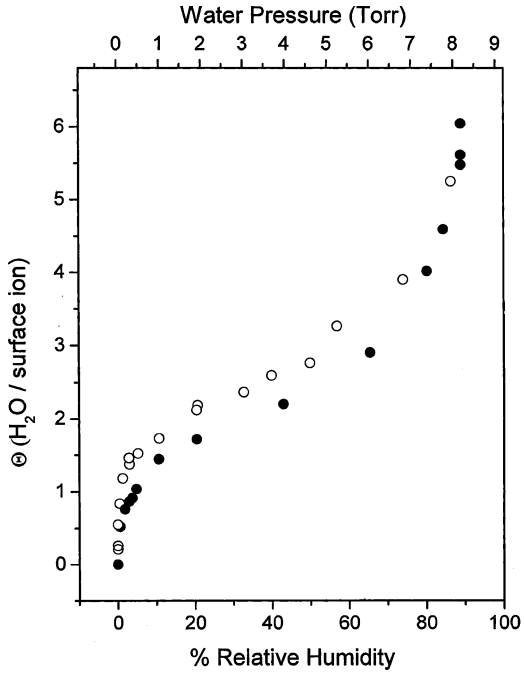

Figure 14. Isotherm for water on MgO(001) at 10 °C. Reproduced with permission from ref 108. Copyright 2005 Elsevier.

evident with the closed circles for coverages obtained at increasing pressures and the open circles for decreasing pressures.

This isotherm, as distinct from the ones we have examined for H_2O/NaCl(001) and H_2O/mica (001), is of a shape that closely resembles that of the BET form in Figure 3. This behavior suggested to Foster et al. that the film grows by way of three-dimensional island formation.[108] Using a family of isotherms over a temperature range −10 to 40 °C the enthalpy of adsorption was determined to be about −60 kJ mol^{-1} for $\Theta = 1$, approaching that of neat water, −44 kJ mol^{-1}, above $\Theta = 3$.

It remains to discuss the deflection near 3700 cm^{-1} in the H_2O/MgO(001) spectra. The assignment to the absorption of OH^- bound to the surface seems likely. To begin, the reaction of MgO with water vapor to produce $Mg(OH)_2$ is thermodynamically favored with $\Delta G_r^\circ = -35.5$ kJ mol^{-1}. The otherwise smooth MgO(001) surface exposed to water vapor at 25 mbar for 100 h at room temperature reveals the growth of micrometer-size patches up to 0.1 μm high when interrogated with AFM,[107] suggesting some surface reactions. The infrared spectrum of MgO powder exposed to an atmosphere with 100% RH shows a sharp feature at 3700 cm^{-1} attributed to absorption by hydroxyls on the crystallite faces.[106] The odd shape of the infrared signature near 3700 cm^{-1} has a precedent. In their infrared study of OH^- formed at defect sites on NaCl crystallites, Dai et al. detected an absorption centered near 3667 cm^{-1}.[109] When the OH^- containing surface was covered by an adlayer of hydrogen molecules, a slight shift in frequency occurred. The ratio of the adlayer shifted absorption with the original absorption gave a sigmoid feature: a negative going absorbance near 3670 cm^{-1} and a positive going absorbance near 3664 cm^{-1}. In Figure 13, the negative going feature at 3720 cm^{-1} and the shoulder (positive going feature) near 3680 cm^{-1} reveal a signature resembling that found for OH^- on NaCl. Thus there is evidence for OH^- on MgO(001) as well.

What is not settled in the discussion of thin film water on MgO(001) is to what extent the oxide surface has been hydroxylated. Thermodynamics ensures us of complete hydroxylation; it is a question of kinetics of how long this will take.

The presence of OH^- ions at the surface of MgO are a type of substitutional defect. This defect will have associated with it, among other things, a characteristic electric field that will alter water adsorption. Other defects, adatoms, vacancies, steps, etc., will likewise alter the nature of water adsorption and thin film formation.

5.4. $H_2O/BaF_2(111)$

Barium fluoride, like NaCl and MgO, has a face-centered cubic structure, but unlike these ionic crystals, its low-energy surface is (111).[110] This surface exposes a hexagonal array of barium and fluoride ions whose lattice constant matches that of the basal face of ordinary I_h ice to within a few percent.[111] This structural coincidence has motivated exploration of the efficacy of BaF_2 surfaces as an ice nucleation agent.[112] The logic can be traced to the work of Bernard Vonnegut who searched the crystallographic literature for morphological matches of inorganic solids with ice. One of these matches, silver iodide in the form of a smoke of crystallites, was found to be particularly successful in cloud seeding.[113] However a variety of other substances including testosterone,[114] certain bacteria,[115] and pulverized leaves,[116] whose morphological connection with ice is not apparent, are also effective in ice nucleation. Nevertheless it has been demonstrated repeatedly that surfaces that have lattice constants close to that of ice facilitate growth in the form of hexagonal platelets.[117]

Many of the investigations of water on $BaF_2(111)$ have employed UHV techniques. An X-ray photoelectric spectroscopic study found evidence that water adsorbs dissociatively on the surface, with the replacement of F^- by OH^-. Defect sites were proposed as reaction centers.[118] Helium atom scattering (HAS) found a (1×1) monolayer H_2O structure formed at 130 K, which disappeared on warming to room temperature.[119] A theoretical study by Nutt and Stone[120] using methods we have already described determined effective charges of $+1.6$ for Ba^{2+} and -0.8 for F^-. They found a single water molecule positioned with its oxygen near the barium ion and its hydrogens toward nearby fluoride ions.

We move now to consider ambient temperature experiments and calculations. Second harmonic generation (SHG) measurements suggested pseudomorphous epitaxial growth of water on $BaF_2(111)$.[121] A molecular dynamics calculation using a simple potential found evidence for the growth of I_h ice.[122] Atomic force microscopy (AFM) measurements on thin film water on $BaF_2(111)$[123] were reminiscent of the observations of water on mica (001). For the generation of thin film isotherms and thermodynamic properties, we turn to an infrared study by Sadtchenko et al.[124]

The technique is identical to that already described for water adsorption on NaCl(001), mica (001), and MgO(001). Absorption spectra of H_2O adlayers on $BaF_2(111)$ at 25 °C for various pressures are shown in Figure 15. At the lowest

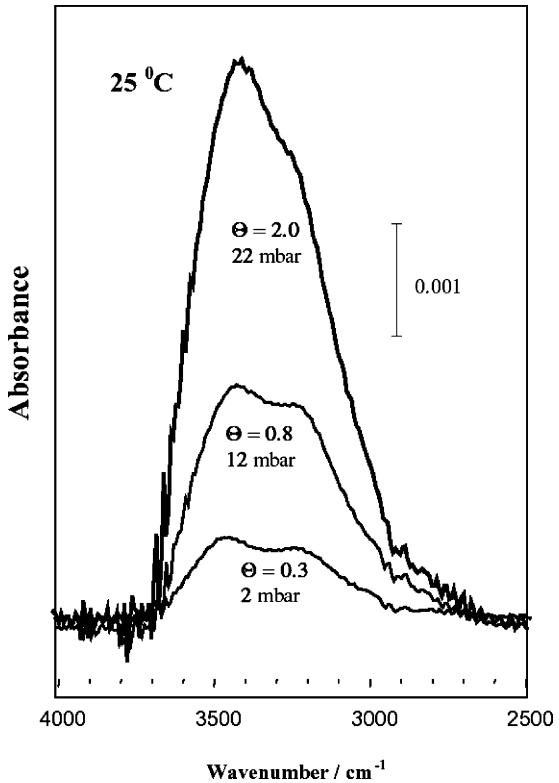

Figure 15. Infrared spectra of thin film water on $BaF_2(111)$. Reproduced with permission from ref 124. Copyright 2002 American Institute of Physics.

pressure, 2 mbar, the spectrum reveals a diffuse doublet. A pressure increase to 12 mbar produces a nearly 3-fold increase in absorbance but only a subtle change in the doublet profile. Finally, in the upper spectrum, a pressure increase by 10 mbar has produced an increase in absorbance by more than a factor of 2. The resulting diffuse profile at 22 mbar, no longer a doublet, is centered at 3400 cm^{-1} with an ill-defined shoulder near 3200 cm^{-1}. Disregarding the shoulder, the band center and high frequency side of this profile closely resembles that of liquid water, see Figure 4.

Consider first the doublet profiles of the 25 °C lower coverage spectra represented in Figure 15. To begin, these spectra do not resemble the diffuse singlet spectroscopic signature of liquid water. Nor do they resemble the spectra of monolayer water on NaCl(001) represented by a broad asymmetric band located near 3420 cm^{-1} (Figure 4) and associated with a disordered two-dimensional hydrogen-bonded network (Figure 1). Since there are two distinct features in the infrared spectrum of submonolayer water on $BaF_2(111)$, it was argued that, unlike the thin films on NaCl-(001), this adlayer is consistent with an ice-like bilayer even at ambient temperature. This interpretation is favored by the molecular dynamics (MD) calculations of Wassermann et al.[122] at 27 °C, who find an ice-like bilayer bound to $BaF_2(111)$. The bilayer may be viewed as a lattice of buckled six-membered rings of H_2O molecules interconnected by hydrogen bonds. (The oxygen framework of the buckled six-membered rings of H_2O is of the same symmetry as the carbon framework in the chair form of cyclohexane.) Devlin and Buch have calculated the spectrum of the bilayer at the surface of an ice cluster.[125] The infrared profile of a bilayer of water molecules on a structurally matched substrate, that is, $BaF_2(111)$, is likely to resemble the top bilayer on the basal face of an ice crystal. The principle difference for BaF_2-(111) is that the lone pair in the lower layer is directed to a Ba^{2+} ion below, while in the ice case it is directed toward a proton to which it hydrogen bonds. The calculation of Devlin and Buch is for the infrared spectrum of a D_2O ice bilayer at the surface of a 450 molecule cluster. To compare these calculations to the H_2O bilayer, each vibrational frequency was scaled by a factor to correct for the H and D mass difference. A comparison of the calculated ice-like H_2O bilayer with the $\Theta = 0.8$ spectrum of Figure 15 showed reasonable agreement. An ice-like adlayer at temperatures above the bulk-ice melting point can be rationalized since the interactions of H_2O molecules with the substrate are strong. As a consequence, the order is preserved in the adlayer at temperatures above the ice melting point because H_2O molecules are immobilized at the adsorption sites.

Having argued that an ordered, ice-like bilayer of H_2O molecules forms on the $BaF_2(111)$ surface at submonolayer and monolayer coverages, Sadtchenko et al. found it easy to explain the spectral variation at $\Theta = 2$. The spectrum of such a liquid-like, disordered adlayer must be similar to spectra of bulk liquid water. The two-band structure that is present in the spectra at low H_2O coverages disappears, and a broad asymmetric peak centered at 3400 cm^{-1} is observed. As already mentioned, the profile at higher coverages is similar to the spectra of neat water with one exception. An ill-defined shoulder near 3200 cm^{-1} contributes significantly to the overall bandwidth. Some contrast between spectra of neat water and the spectra of high-coverage H_2O adlayers, however, is expected. It is possible that unlike water, the multilayer H_2O films may not be completely disordered. Water molecules that are close to the surface of $BaF_2(111)$ must be influenced by the substrate in such a way that their entropy is slightly lower than the entropy of the molecules further from the substrate. The shoulder at 3200 cm^{-1}, whose frequency is the signature for ice,[126] may be a manifestation of the residual ordering of the surface bound H_2O adlayer in the case of high coverages.

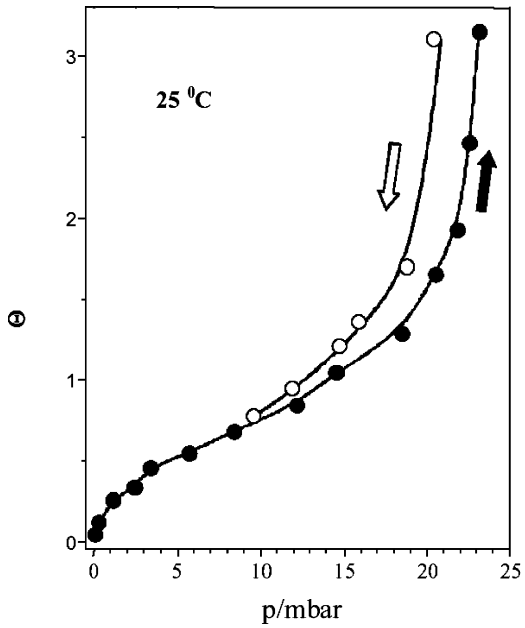

Figure 16. Isotherms of water on $BaF_2(111)$. Adsorption is indicated by up arrow, desorption by down arrow. Reproduced with permission from ref 124. Copyright 2002 American Institute of Physics.

The isotherms in Figure 16 further reveal the nature of water adlayers on $BaF_2(111)$.[124] Recalling the statistical nature of adsorption for systems under ambient conditions, for the coverage stated to be $\Theta = 1$, the bilayer actually will not be complete but consist of islands with their upper layers partially covered by adsorbed molecules. Now consider the interpretation of the low-coverage region, $\Theta < 0.5$, of the isotherm below 5 mbar. The spectroscopic signatures suggest small islands. Presumably these low coverages correspond to an equilibrium at the $BaF_2(111)$ surface between a two-dimensional gas of H_2O molecules and two-dimensional ice-like islands. The absorptions of isolated adsorbed H_2O molecules (the two-dimensional gas) are presumably too weak to be detected because of both their low concentration and low optical cross sections.

The adsorption and desorption isotherms are irreversible at coverages above $\Theta = 1$ as shown in Figure 16. Having interpreted the variations in the spectra in Figure 15 as evidence for disordering of the ice-like adlayer by adsorption of water molecules on top of it, Sadtchenko using a kinetic argument showed that the hysteresis in the isotherm at 25 °C further supports this conclusion.

Hysteresis in the isotherm demonstrates that, depending on their history, two H_2O films of identical thickness may have different vapor pressures above their surfaces. Therefore, the observed isotherm hysteresis suggests that significant variations occur in the structure of the adlayer when the film thickness exceeds some critical value between one and two monolayers. As they proposed, the variations in the structure of the H_2O adlayer may consist in transition from highly ordered hexagonal to liquid-like disordered structure as the coverage increases above $\Theta = 1$. The disordering of the thin ice-like adlayer covered by a liquid-like film must be a kinetic process that is probably complete on the time scale of their experimental measurement (10−20 min). Miura et al. have studied the kinetics of water adsorption on a $BaF_2(111)$ surface at room temperature by AFM near 22 mbar.[123] According to these results, the adsorption of a $\Theta = 1$ film was followed by formation of droplets with small contact angles. However the droplets eventually disappeared resulting in a multilayer film. This observation is in accord with the conclusion about the nature of variations in the adlayer structure during multilayer adsorption attributed to the spectrum changes in the range from 12 to 22 mbar. Indeed, a phase separation must occur initially after adsorption of H_2O molecules on the top of the ice-like adlayer that may manifest itself as liquid drops. The uniform liquid-like film is observed when the disordering of the ice-like layer is complete.

Enthalpy and entropy of H_2O adsorption on the $BaF_2(111)$ surface have been derived from the isotherms spanning the temperatures −1 to 25 °C. The condensation of water onto $BaF_2(111)$ is exothermic at all coverages. At the lowest submonolayer coverages, the adsorption enthalpy becomes the least exothermic. Indeed at $\Theta = 0.2$ the enthalpy is −38 kJ mol^{-1}, which is a significant departure from the value for liquid water. As suggested, the adsorption of H_2O on $BaF_2(111)$ initially proceeds with formation of small islands with a large number of incompletely coordinated H_2O molecules on the periphery. At the island edges, the lack of neighbor molecules with which to form hydrogen bonds must result in a low value of adsorption bonding. As more water molecules adsorb to approach monolayer coverage, the islands begin to coalesce. The resulting adlayer is characterized by an extended network of lateral hydrogen bonds and therefore, the adsorption enthalpy is more exothermic. Indeed, the adsorption enthalpy is most exothermic at $\Theta = 0.8$. The exothermic extremum of −58 kJ mol^{-1} is significantly lower than the enthalpy of condensation of either ice (−48 kJ mol^{-1}) or liquid water (−44 kJ mol^{-1}). This value also suggests that the interactions of H_2O molecules with the $BaF_2(111)$ surface are strong. The enthalpy of adsorption measured at coverages close to $\Theta = 1$ supports the conclusion that H_2O adsorption on $BaF_2(111)$ leads to the formation of an ordered layer "nailed" to the substrate.

At H_2O coverages above $\Theta = 1$, the enthalpy of adsorption decreases significantly and approaches the enthalpy of adsorption of bulk liquid water. The change in the adsorption enthalpy from −58 to − 44 kJ mol^{-1} is in agreement with the proposed transition from ordered to disordered, liquid-like structure of the H_2O adlayer on $BaF_2(111)$ surface at multilayer coverages.

The variation in entropy of adsorption with coverage mirrors the change in enthalpy. At low coverage, the entropy of the H_2O adlayer on BaF_2 is actually higher than the entropy of bulk water. This may arise because many islands containing small numbers of water molecules contribute configuration entropy. Furthermore, the desorption of water molecules is likely to occur via a two-step mechanism resulting in a large number of mobile desorption precursors, essentially H_2O monomers, on the substrate surface.[127] As the coverage increases, the entropy of the adlayer decreases rapidly, achieving a minimum value of about 40 J K^{-1} mol^{-1} near $\Theta = 1$, which is significantly lower than the entropy of liquid water. Note that the corresponding $\Theta = 1$ entropy value for water on mica (001) is somewhat higher (Figure 9), suggesting again that this substrate does not favor an ice-like adlayer.

At H_2O coverages above $\Theta = 1$, the entropy of the adlayer approaches 68 J K^{-1} mol^{-1}, near the value for water of 70 J K^{-1} mol^{-1}.[48] The increase in entropy from 40 to 68 J K^{-1} mol^{-1} at multilayer coverages is in agreement with the proposed transition from ice-like to liquid-like structure of the H_2O adlayer on $BaF_2(111)$ surface.

Another important conclusion follows directly from these adsorption measurements. Since the enthalpy of adsorption at $\Theta = 3$ coverage is equal to the adsorption enthalpy of H_2O on the surface of liquid water, it is unlikely that the interactions of H_2O molecules with ions of BaF_2 substrate propagate through a distance greater than a few H_2O molecular diameters. This conclusion is consistent with the findings[30,33] for thick films of water on NaCl(001) and mica (001).

In their interpretations of low coverage thin film water on $BaF_2(111)$ as ice-like, Sadtchenko et al.[124] later would make a distinction between "ice" and "ice-like". The molecular simulation by Nutt and Stone[120] showed that the six-molecular buckled hexagonal ring of H_2O molecules, a building block for ordinary I_h ice, was not a stable structure on $BaF_2(111)$. A disordered bilayer structure was found to be a stable low coverage form of water. The experiments and theoretical interpretations of Sadtchenko et al.[128] actually showed that an ice film was unstable on $BaF_2(111)$. Conrad et al.[112] found that thin film water required supercooling to −30 °C before freezing occurred.

5.5. H_2O/α-$Al_2O_3(0001)$

Crystalline α-$Al_2O_3(0001)$ of high purity is commercially available and can be cut and polished to expose (0001) faces.[129] Scratches or pits left from the polishing can be annealed away by high-temperature treatment to produce an atomically flat (ultrasmooth) surface.[130] The (0001) face is strained since the tetrahedral bonding of the aluminum atoms to their oxygen partners in the interior of the crystal has been broken in preparing the surface. These dangling bonds are available to reaction, and exposure to water causes the surface to be hydroxylated and be transformed into −OH groups.[131] The surface region is chemically better described by $Al(OH)_3$ rather than Al_2O_3. There are a variety of recipes for preparing the surface of α-Al_2O_3 crystals, and the researcher needs to be careful which procedure to follow.

Early studies of water adsorption on α-Al_2O_3 used powders (ground up crystals).[132] But in these experiments, the variety of crystallite surfaces exposed, the presence of defects, and the complex nature of adsorption and desorption kinetics in a porous medium[133] have made analysis difficult. Eng et al.[131] have examined the structure of hydrated α-$Al_2O_3(0001)$ surface using a synchrotron X-ray source. A highly polished single-crystal wafer of α-$Al_2O_3(0001)$ was treated under stringent conditions. On exposure of the wafer to water vapor at 27 °C, their analysis showed a structure intermediate between α-Al_2O_3 and the fully hydroxylated γ-$Al(OH)_3$ form of alumina.

Al-Abadieh and Grassian[34] have recently studied thin film water on single-crystal α-Al_2O_3 using infrared absorption spectroscopy. The single wafers they used were heated in air to 500 °C but were not otherwise treated. Presumably some (complete) hydroxylation at the crystal surfaces took place. Adapting the technique developed by Ewing's group,[29] they measured the infrared absorption on these crystal surfaces as a function of relative humidity to produce the isotherm shown in Figure 17. Notice that the coverage, which is approaching $\Theta = 8$ near 100% RH, is much higher than any of the previous systems we have reviewed. The S-shape of the isotherm resembles that of the BET form (see Figure 3), as they point out.

The infrared signatures of adsorbed water on their crystal surfaces contain a number of features in common with

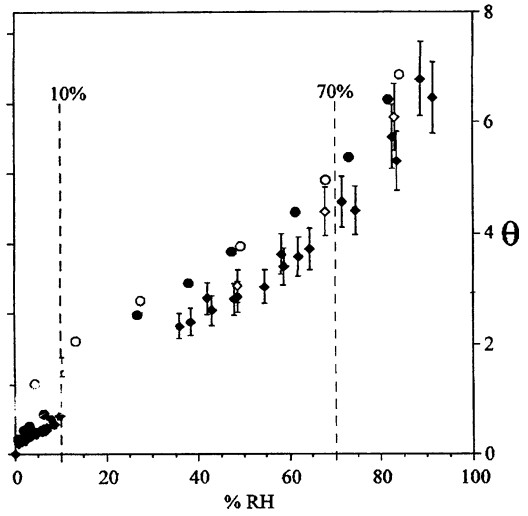

Figure 17. Isotherms of water on α-$Al_2O_3(0001)$ at 23 °C. Circles are for water adsorption on calcined sapphire. Diamonds are for adsorption on sapphire previously exposed to water and stored at 413 K for 24 h. Filled symbols are for increasing pressure and open symbols for decreasing pressure. Reproduced with permission from ref 34. Copyright 2003 American Chemical Society.

spectra we have discussed. A negative going absorbance near 3700 cm^{-1} resembles an analogous feature observed for H_2O on MgO(001) tentatively assigned to chemically bonded −OH groups. A diffuse doublet near 3300 and 3400 cm^{-1} observed near monolayer coverage is suggestive of a similar doublet in the H_2O on the $BaF_2(111)$ system shown in Figure 15. Al-Abadieh and Grassian use this structure to suggest an ordering of low-coverage adsorbed water molecules.

6. The End Game

How should the study of thin film water approach its conclusion? We begin by trying to identify some patterns in the five systems reviewed.

Since the topic is ambient thin film water, let us consider the film thickness at room temperature and a relative humidity of 50%. We use data available from the various studies and calculate the thickness, h, from coverage values, Θ, using eq 1. We find 0.5 nm for NaCl(001),[30] 0.4 nm for mica (001),[81] 1 nm for MgO(001),[106] 0.4 nm for $BaF_2(111)$,[124] and 1 nm for α-$Al_2O_3(0001)$.[34] Using $\rho_w^{-1/3} = 0.31$ nm for a monolayer slice of bulk water, we find then coverages ranging from one to three for ambient thin film water on these insulator surfaces.

The thermodynamic measurements are available for all but the α-$Al_2O_3(0001)$ surface. If we make the comparisons for monolayer coverage, $\Theta = 1$, we find the most exothermic value for MgO(001) at −60 kJ mol^{-1} [108] and the least for NaCl(001) at −50 kJ mol^{-1},[30] all values significantly more exothermic than the enthalpy of condensation of neat water of −44 kJ mol^{-1}. The most ordered monolayer of those measured corresponds to an entropy of 40 J K^{-1} mol^{-1} for the film on $BaF_2(111)$.[124] This value is even lower than that of ice. The convergence of the thermodynamic values of the film to that of neat water corresponds to about $\Theta = 3$ for NaCl(001),[30] mica (001),[39] and $BaF_2(111)$.[124]

There is no obvious pattern in the shapes of the isotherms. The form of the BET isotherm roughly coincides with the MgO(001), $BaF_2(111)$, and α-$Al_2O_3(0001)$ isotherms. No successful interpretation of the mica (001) isotherm has been made. The complex behavior of the H_2O/NaCl(001) isotherm

has been interpreted as a 2-D to 3-D phase transition, which then converges to its deliquescence behavior.

The qualitative distinction in the infrared absorption profiles in the −OH stretching region for ice and liquid water[83,84] allow some inferences to be made about the hydrogen bonding networks in thin film water. "Ice-like" structures have been proposed for monolayer water on mica (001) and BaF_2(111). In all cases, the band profile approaches that of neat water at coverages of several molecular layers.

What can be said about the evacuated substrate after the introduction of water vapor? In all cases where data is available, there is a change. There is step migration on NaCl(001),[67] patches form on MgO(001),[107] the anion on mica (001) becomes solvated, and α-Al_2O_3(0001) undergoes hydroxylation.[131] It is likely that the surface of BaF_2(111) becomes pitted.[112]

The nature of the water/vapor interface is being explored by nonlinear optical spectroscopies and molecular simulations.[134] But the influence of a nearby substrate on the thin film/vapor interface needs investigation.

For the optical interrogation of the entire film, as opposed to only the interfaces that nonlinear spectroscopies can explore, the method developed by Zhang and Ewing[135] shows promise. With use of a prism of the substrate to be investigated, attenuated partial reflection that penetrates the entire film can determine water molecular orientation. Other substrate geometries can also be used.[136]

Other systems need study. Investigations of the properties of silica in its crystalline (e.g., quartz) or amorphous forms (e.g., various glasses) as supporters of thin film water have only just begun.[137−140] Organic polymer insulators are ripe for study.

We are only at the early stage of the end game.

7. Acknowledgments

A long time collaborator has been Anthony Stone who, with his group, has pioneered important molecular simulation methods for the study of thin film water. Recent valuable correspondence with Jianwei Wang and Miguel Salmeron is acknowledged. Our study of the infrared spectroscopy of thin film water began with Steve Peters and continued with Shelley Foster, Zhenfeng Zhang, Will Cantrell, Vlad Sadtchenko, Peter Conrad, Charles McCrory, and Rob Karlinsey. Many of their experiments, their ideas, and even their words have appeared in this review. Thank you all. Finally the continued support of The National Science Foundation is acknowledged.

8. References

(1) Ewing, G. E. *J. Phys. Chem. B* **2004**, *108*, 15953.
(2) Warneck, P. *Chemistry of the Natural Atmosphere*; Academic Press: San Diego, CA, 1988.
(3) DeHann, D. O.; Brauers, T.; Oum, K.; Stutz, J., Nordmeyer, T.; Finlayson-Pitts, B. J. *Int. Rev. Phys. Chem.* **1999**, *18*, 343.
(4) Pruppacher, H. R.; Klett, J. D. *Microphysics of Clouds and Precipitation*; Kluwer Academic Publishers: Dordrecht, The Netherlands, 1997.
(5) *Kirk-Othmer Encyclopedia of Chemical Technology*; Wiley: New York, 2000.
(6) Tardos, G. I.; Nicolaescu, I. V.; Ahtchi-Ali, B. *Powder Handl. Process.* **1996**, *8*, 7.
(7) Allen, H. C.; Laux, J. M.; Vogt, R.; Finlayson-Pitts, B. J.; Hemminger, J. C. *J. Phys. Chem.* **1996**, *100*, 6371.
(8) Stumm, W.; Sigg. L.; Sulzberger, B., *Chemistry of the Solid-Water Interface*: *Processes at the Mineral-Water and Particle−Water Interface in Natural Systems*; Wiley: New York, 1992.
(9) Faraday, M. Royal Institution Discourse, June 7, 1850. *Experimental Researches in Chemistry and Physics*; Taylor and Francis: New York, 1991.
(10) Dash, J. G.; Mason, B. L.; Wettlaufer, J. S. *J. Geophys. Res.* **2001**, *106*, 20395.
(11) Rempel, A. W.; Waddington, E. D.; Wettlaufer, J. S.; Worster, M. G. *Nature* **2001**, *411*, 568.
(12) Dash, J. G.; Fu, H.-Y.; Wettlaufer, J. S. *Rep. Prog. Phys.* **1995**, *58*, 115.
(13) Conklin, M. H.; Bales, R. C. *J. Geophys. Res.* **1993**, *98*, 16851.
(14) Peter, T. *Annu. Rev. Phys. Chem.* **1997**, *48*, 785.
(15) Dash, J. G. *Rev. Mod. Phys.* **1999**, *71*, 1737.
(16) Brown, G. E.; Henrich, V. E.; Casey, W. H.; Clar, D. L.; Eggleston, C.; Felmy, A.; Goodman, D. W.; Gratzel, M.; Maciel, G.; McCarthy, M. I.; Nealson, K. H.; Sverjensky, D. A.; Toney, M. F.; Zachara, J. M. *Chem. Rev.* **1999**, *99*, 77.
(17) Langmuir, I. *J. Am. Chem. Soc.* **1918**, *40*, 1361.
(18) Thiel, P. A.; Madey, T. E. *Surf. Sci. Rep.* **1987**, *7* (6−8), 211.
(19) Henderson, M. A. *Surf. Sci. Rep.* **2002**, *46* (1−8), 1.
(20) Bruch, L. W.; Glebov, A.; Toennies, J. P.; Weiss, H. *J. Chem. Phys.* **1995**, *1103*, 5109.
(21) Derjaguin, B. V.; Churaev, N. V.; Muller, V. M. In *Surface Forces (Translation from Russian)*; Kisin, V. I., Kitchener, J. A., Eds.; Consultants Bureau: New York, 1987.
(22) Israelachvili, J. N. *Intermolecular and Surface Forces*; Academic Press: London, 1985.
(23) Shindo, H.; Ohashi, M.; Tateishi, O.; Seo, A. *J. Chem. Soc., Faraday Trans.* **1992**, *93*, 1169.
(24) Hu, J.; Xias, X.-D.; Ogletree, D. F.; Salmeron, M. *Science* **1995**, *268*, 267.
(25) Elbaum, M.; Lipson, S. G.; Dash, J. G. *J. Cryst. Growth* **1993**, *129*, 491.
(26) Beaglehole, D.; Nason, D. *Surf. Sci.* **1980**, *96*, 363.
(27) Furukawa, Y.; Yamamoto, M.; Kuroda, S. *J. Cryst. Growth* **1987**, *82*, 665.
(28) Beaglehole, D.; Radlinska, W. Z.; Ninham, B. W.; Christenson, H. K. *Phys. Rev. Lett.* **1991**, *66*, 2084.
(29) Peters, S. J.; Ewing, G. E. *J. Phys. Chem. B* **1997**, *101*, 10880. Peters, S. J.; Ewing, G. E. *Langmuir* **1997**, *13*, 6345.
(30) Foster, M.; Ewing, G. E. *J. Chem. Phys.* **2000**, *112*, 6817.
(31) Ewing, G. E.; Foster, M.; Cantrell, W.; Sadtchenko, V. Thin Film Water on Insulator Surfaces. In *Water in Confining Geometries*; Buch, V., Devlin, J. P., Eds.; Springer-Verlag: Berlin, 2003; p 179.
(32) Sadtchenko, V.; Conrad, P.; Ewing, G. E. *J. Chem. Phys.* **2002**, *116*, 4293.
(33) Cantrell, W.; Ewing, G. E. *J. Phys. Chem. B* **2001**, *105*, 5434.
(34) Al-Abadleh, H. A.; Grassian, V. H. *Langmuir* **2003**, *19*, 341.
(35) Shang, X.; Benderskii, A. V.; Eisenthal, K. B. *J. Phys. Chem. B* **2001**, *105*, 11578.
(36) Shen, Y. R. *Solid State Commun.* **1998**, *108*, 399.
(37) Shultz, M. J.; Schnitzer, C.; Simonelli, D.; Baldelli, S. *Int. Rev. Phys. Chem.* **2000**, *19*, 123.
(38) Becraft, K. A.; Richmond, G. L. *Langmuir* **2001**, *17*, 7721.
(39) Engkvist, O.; Stone, A. J. *J. Chem. Phys.* **2000**, *112*, 6827.
(40) Döppenschmidt, A.; Butt, H.-J. *Langmuir* **2000**, *16*, 6709.
(41) Wassermann, B.; Reif, J.; Matthuias, E. *Phys. Rev. B* **1994**, *50*, 2593.
(42) Furukawa, Y.; Nada, H. *J. Phys. Chem. B* **1997**, *101*, 6167.
(43) Kroes, G.-J. *Surf. Sci.* **1992**, *275*, 365.
(44) Gibbs, J. W. *The Collected Works of J. Willard Gibbs*; Longmans, Green and Co.: New York, 1928.
(45) Drude, P. *The Theory of Optics*; Longmans, Green and Co.: New York, 1902.
(46) *National Research Council (US) International Critical Tables*; McGraw-Hill: New York, 1926.
(47) Stone, A. J. *The Theory of Intermolecular Forces*; Clarendon Press: Oxford, U.K., 1997.
(48) Atkins, P. *Physical Chemistry*, 6th ed; WH Freeman: New York, 1998.
(49) Lennard-Jones, J. F.; Dent, B. M. *Trans. Faraday Soc.* **1928**, *24*, 92.
(50) Engkvist, O.; Stone, A. J. *J. Chem. Phys.* **1999**, *110*, 12089.
(51) Henderson, D.; Abraham, F. A.; Barker, J. *Mol. Phys.* **1976**, *31*, 1291.
(52) Lee, C. Y.; McGammon, S. A.; Rossky, P. J. *J. Chem. Phys.* **1984**, *80*, 4448.
(53) Noda, C.; Ewing, G. E. *Surf. Sci.* **1990**, *240*, 181.
(54) Hill, T. L. *Introduction to Statistical Thermodynamics*; Addison-Wesley: Reading, MA, 1960.
(55) Berg, O.; Ewing, G. E. *Surf. Sci.* **1989**, *220*, 207.
(56) Dash, J. *Phys. Rev. B* **1977**, *15*, 3136.
(57) Bassett, C. A. *Philos. Mag.* **1958**, *3*, 1042.
(58) Meyer, G.; Amer, N. M. *Appl. Phys. Lett.* **1990**, *56*, 2100; **1990**, *57*, 2089.
(59) Schuger, A. L.; Wilson, R. M.; Williams, R. T. *Phys. Rev.* **1994**, *B49*, 4915.

(60) Fölsch, A.; Stock; Henzler, M. *Surf. Sci.* **1992**, *65*, 264.
(61) Barraclough, P. B.; Hall, P. G. *Surf. Sci.* **1974**, *46*, 393.
(62) Walter, H. U. *Z. Phys. Chem.* **1971**, *75*, 287.
(63) Lad, R. A. *Surf. Sci.* **1968**, *12*, 37.
(64) Kaiho, M.; Chikazawa, M.; Kanazawa, T. *Nippon Kagahu Kashi* **1972**, *8*, 1368.
(65) Querry, M. R.; Waring, R. C.; Holland, W. C.; Hale, G. M.; Nijm, W.
(66) Downing, H. D.; Williams, D. *J. Geophys. Res.* **1975**, *80*, 1656.
(67) Hucher, M.; Oberlin, A.; Hobast, R. *Bull. Soc. Fr. Mineral. Cristallogr.* **1967**, *90*, 320.
(68) Shindo, H.; Ohashi, M.; Tateishi, O.; Seo, A. *J. Chem. Soc., Faraday Trans.* **1992**, *93*, 1169.
(69) Hu, J.; Xiao, X.-D.; Ogletree, D. F.; Salmeron, M. *Science* **1995**, *268*, 267.
(70) Hu, J.; Xiao, X.-D.; Ogletree, D. F.; Salmeron, M. *Appl. Phys. Lett.* **1995**, *67*, 476.
(71) Xu, L.; Lio, A.; Hu, J.; Ogletree, D. F.; Salmeron, M. *J. Phys. Chem. B* **1998**, *102* (3), 540.
(72) Luna, M.; Rieutord, F.; Melman, N. A.; Dai, Q.; Salmeron, M. *J. Phys. Chem. A* **1998**, *102*, 6793.
(73) Verdaguer, A.; Sacha, G. M.; Luna, M.; Ogletree, D. F.; Salmeron, M. *J. Chem. Phys.* **2005**, *123*, No. 124703.
(74) Pauling, L. *The Nature of the Chemical Bond*, 3rd ed.; Cornell University Press: New York, 1960.
(75) Schmid, E.; Boas, W. *Plasticity of Crystals*; Chapman and Hall: London, 1968.
(76) Turnbull, D.; Vonnegut, B. *Ind. Eng. Chem.* **1952**, *44*, 1292.
(77) Jaffray, J.; Montmory, R. *C. R. Acad. Sci. (Paris)* **1957**, *245*, 2221.
(78) Bryant, G.; Hallett, J.; Mason, B. *J. Phys. Chem. Solids* **1959**, *12*, 189.
(79) Beaglehole, D.; Radlinska, E.; Ninham, B.; Christenson, H. K. *Phys. Rev. Lett.* **1991**, *66*, 2084.
(80) Beaglehole, D.; Christenson, H. K. *J. Phys. Chem.* **1992**, *96*, 3395.
(81) Miranda, P.; Xu, L.; Shen, Y.; Salmeron, M. *Phys. Rev. Lett.* **1998**.
(82) Elbaum, M.; Lipson, S. G. *Phys. Rev. Lett.* **1994**, *72*, 3562.
(83) Pimental, G.; McClellan, A. *The Hydrogen Bond*; Reinhold: New York, 1960.
(84) Eisenberg, D.; Kauzmann, W. *The Structure and Properties of Water*; Oxford: New York, 1969.
(85) Beaglehole, D. *Physica A* **1997**, *244*, 40.
(86) Odelius, M.; Bernasconi, M.; Parrinello, M. *Phys. Rev. Lett.* **1997**, *78*, 2855.
(87) Xu, L.; Liu, A.; Hu, J.; Ogletree, D. F.; Salmeron, M. *J. Phys. Chem. B* **1998**, *102*, 540.
(88) Wang, J.; Kalinichev, A. G.; Kirkpatrick, R. J.; Cygan, R. T. *J. Phys. Chem. B* **2005**, *109*, 15893.
(89) Henrich, V. E.; Cox, P. A. *The Surface Science of Metal Oxides*; Cambridge University Press: Cambridge, U.K., 1996.
(90) Grassian, V. H. *Int. Rev. Phys. Chem.* **2001**, *20*, 467.
(91) Tikhomirov, V. A.; Geudnter, G.; Jug, K. *J. Phys. Chem. B* **1997**, *101*, 10398.
(92) Johnson, M. A.; Stevanovich, E. V.; Truong, T. N. *J. Phys. Chem.* **1998**, *102*, 6391.
(93) Engkvist, O.; Stone, A. J. *Surf. Sci.* **1999**, *437*, 239.
(94) Marmier, A.; Hoang, P. N. M.; Picaud, S.; Girardet, C.; Lynden-Bell, R. M. *J. Chem. Phys.* **1998**, *109*, 3245.
(95) Girardet, C.; Hoang, P. N. M.; Marmier, A.; Picaud, S. *Phys. Rev. B* **1998**, *57*, 11.
(96) Heidberg, J.; Redlich, B.; Wetter, D. *Ber. Bunsen-Ges. Phys. Chem.* **1995**, *99*, 1333.
(97) Xu, C.; Goodman, D. W. *Chem. Phys. Lett.* **1997**, *265*, 341.
(98) Ferry, D.; Picaud, S.; Hoang, P. N. M.; Girardet, C.; Geordano, L.; Demirdjian, B.; Suzanne, J. *Surf. Sci.* **1998**, *409*, 101.
(99) Gunster, J.; Krischok, S.; Stultz, J.; Goodman, D. W. *J. Phys. Chem. B* **2000**, *104*, 7977.
(100) Liu, P.; Kendelewicz, T.; Brown, G. E., Jr.; Parks, G. A. *Surf. Sci.* **1998**, *412/413*, 287.
(101) Abriou, D.; Jupille, J. *Surf. Sci.* **1999**, *430*, L527.
(102) Johnson, M. A.; Stefanovich, E. V.; Truong, T. N.; Gunster, J.; Goodman, D. W. *J. Phys. Chem. B* **1999**, *103*, 3391.
(103) Soria, E.; de Segovia, J. L.; Colera, I.; Gonzalez, R. *Surf. Sci.* **1997**, *390*, 140.
(104) Kim, Y. D.; Lynden-Bell, R. M.; Alavi, A.; Stultz, J.; Goodman, D. W. *Chem. Phys. Lett.* **2002**, *352*, 318.
(105) Kim, Y. D.; Stultz, J.; Goodman, D. W. *J. Phys. Chem. B* **2002**, *106*, 1515.
(106) Foster, M.; Furse, M.; Passno, D. *Surf. Sci.* **2002**, *502*−*503*, 102.
(107) Foster, M.; Passno, D.; Rudberg, J. *J. Vac. Sci. Technol., A* **2004**, *22*, 1640.
(108) Foster, M.; D'Agostina, M.; Passno, D. *Surf. Sci.* **2005**, *590*, 31.
(109) Dai, D.; Peters, S. J.; Ewing, G. E. *J. Phys. Chem.* **1995**, *99*, 10299.
(110) Swanson, H. E.; Tatge, E. *Natl. Bur. Stand. Circ. (U.S.)* **1953**, *70*, 539.
(111) Petrenko, V. F.; Whitworth, R. W. *Physics of Ice*; Oxford University Press: Oxford, U.K., 1999.
(112) Conrad, P.; Ewing, G. E.; Karlinsky, R. L.; Sadtchenko, V. *J. Chem. Phys.* **2005**, *122*, 64709.
(113) Vonnegut, B. *J. Appl. Phys.* **1947**, *18*, 593.
(114) Head, R. B. *Nature (London)* **1961**, *191*, 1058.
(115) Schnell, R. C.; Vali, G. *J. Atmos. Sci.* **1976**, *33*, 1554.
(116) Schnell, R. C.; Schnell-Tan, S. N. *Tellus* **1982**, *34*, 92.
(117) Hobbs, P. V. *Ice Physics*; Clarendon: Oxford, U.K., 1974.
(118) Wu, Y.; Mayer, J. T.; Garfunkel, E.; Madey, T. E. *Langmuir* **1994**, *10*, 1482.
(119) Lehmann, A.; Fahsold, G.; Konig, G.; Rieder, K. H. *Surf. Sci.* **1996**, *369*, 289.
(120) Nutt, D.; Stone, A. J. *J. Chem. Phys.* **2002**, *117*, 800.
(121) Zink, J. E.; Reif, J.; Matthias, E. *Phys. Rev. Lett.* **1992**, *68*, 3595.
(122) Wassermann, B.; Reif, J.; Matthias, E. *Phys. Rev. B* **1994**, *50*, 2593.
(123) Mura, K. *Phys. Rev. B* **1995**, *52*, 7872.
(124) Sadtchenko, V.; Conrad. P.; Ewing, G. E. *J. Chem. Phys.* **2002**, *116*, 4293.
(125) Devlin, J. P.; Buch, V. *J. Phys. Chem.* **1997**, *101*, 6095.
(126) Warren, S. G. *Appl. Opt.* **1984**, *23*, 1206.
(127) Davy, J. G.; Somorjai, G. A. *J. Chem. Phys.* **1991**, *55*, 3624.
(128) Sadtchenko, V.; Ewing, G. E.; Nutt, D. R.; Stone, A. J. *Langmuir* **2002**, *18*, 4632.
(129) Union Carbide Products (Washogal, WA).
(130) Yoshida, K.; Yoshimoto, M.; Sasaki, T.; Ohnishi, T.; Ushiki, T.; Hitomi, J.; Yamamoto, S.; Sigeno, M. *Biophys. J.* **1998**, *74*, 1654.
(131) Eng, P. J.; Trainor, T. P.; Brown, G. E., Jr.; Waychunas, G. A.; Newville, M.; Sutton, S. R.; Rivers, M. L. *Science* **2000**, *288*, 1029.
(132) Goodman, A. L.; Bernard, E. T.; Grassian, V. H. *J. Phys. Chem. A* **2001**, *105*, 6443 and references therein.
(133) Gregg, S. T.; Sing, K. S. W. *Adsorption, Surface Area and Porosity*; Academic Press: New York, 1982.
(134) Jungwirth, P.; Tobias, D. J. *J. Phys. Chem. B* **2001**, *105*, 10468.
(135) Zhang, Z.; Ewing, G. E. *Anal. Chem.* **2002**, *74*, 2578.
(136) Cantrell, W.; Ewing, G. E. *Appl. Spectrosc.* **2002**, *56*, 665.
(137) Saliba, N. P.; Yang, H.; Finlayson-Pitts, B. J. *J. Phys. Chem. A* **2001**, *105*, 10339.
(138) Goodman, A. L.; Underwood, G. M.; Grassian, V. H. *J. Phys. Chem. A* **1999**, *103*, 7217.
(139) Barney, W. S.; Finlayson-Pitts B. J. *J. Phys. Chem. A* **2000**, *104*, 171.
(140) Li, I.; Bandara J.; Shultz, M. J. *Langmuir* **2004**, *20*, 10474.

CR040369X